RECONSTRUCTING HOLOCENE SEA-LEVEL CHANGE FOR THE CENTRAL GREAT BARRIER REEF USING SUBTIDAL FORAMINIFERA

BENJAMIN. P. HORTON[1,8], STEPHEN J. CULVER[2], MICHAEL I. J. HARDBATTLE[3], PIERS LARCOMBE[4], GLENN A. MILNE[5], CATERINA MORIGI[6], JOHN E. WHITTAKER[7] and SARAH A. WOODROFFE[3]

RRH: SUBTIDAL FORAMINIFERA

LRH: HORTON AND OTHERS

[1] Sea Level Research Laboratory, Department of Earth and Environmental Science, University of Pennsylvania, Philadelphia, PA 19104-6316, USA.

[2] Department of Geology, East Carolina University, Greenville, North Carolina 27858, USA.

[3] Department of Geography, University of Durham, South Road, Durham, DH1 3LE, UK.

[4] Centre for Environment, Fisheries and Aquaculture Science, Pakefield Road, Lowestoft, Suffolk, NR33 0HT, UK.

[5] Department of Earth Sciences, University of Durham, South Road, Durham, DH1 3LE, UK

[6] Dipartimento di Scienze del Mare, Università Politecnica delle Marche, Via Brecce Bianche, 60131 Ancona, Italia.

[7] Micropaleontology Research, Department of Palaeontology, The Natural History Museum, London, SW7 5BD, UK.

[8] Correspondence author. E-mail: bphorton@sas.upenn.edu

ABSTRACT

We assessed the utility of subtidal foraminifera to reconstruct Holocene relative sea levels from the central Great Barrier Reef shelf, Australia. We collected contemporary foraminiferal samples from Cleveland Bay and Bowling Green Bay, with water depths from -4.2 m to -48.0 m Australian Height Datum (AHD). The subtidal foraminiferal assemblages were divided into two distinct foraminiferal zones: an inner shelf zone occupied by *Elphidium hispidulum, Pararotalia venusta, Planispirinella exigua, Quinqueloculina venusta* and *Triloculina oblonga*; and a middle shelf zone dominated by *Amphistegina lessonii, Dendritina striata* and *Operculina complanata*. The zonations of the study areas and relative abundances of individual species indicated that the distributions of subtidal foraminifera are related to water depth.

We used the subtidal data to develop a transfer function capable of inferring past water depths of sediment samples from their foraminiferal content. The results indicated a robust performance of the transfer function (r^2_{jack} = 0.90). We produced ten sea-level index points, which revealed an upward trend of Holocene relative sea level from -8.86 ± 4.5 m AHD at 9.3-8.6 cal kyr BP to a mid-Holocene high stand of +1.72 ± 3.9 m AHD at 6.9-6.4 cal kyr BP. Sea level subsequently fell from the highstand to the present-day. The sea-level reconstructions are consistent with geophysical models and previous published data.

INTRODUCTION

The recent transition of the earth system from a glacial to an interglacial state produced a dramatic, global sea-level response. Fairbanks (1989), Chappell and Polach (1991) and Bard and others (1996) created benchmark, late glacial and early Holocene, relative sea-level curves using coral-based sea-level indicators. These suggest that since the Last Glacial Maximum approximately 50 million cubic kilometers of ice melted from the land-based ice sheets (Lambeck and others, 2002), raising sea level in tectonically stable regions that are distant from the major glaciation centers (far-field sites) by ca. 120 m (e.g., Peltier and Fairbanks, 2006). This rapid rise in sea level is attributed to the eustatic contribution, which averaged 10 mm yr^{-1} during the deglaciation but peak rates potentially exceeded 50 mm yr^{-1} during "meltwater pulses" at 19 and 14.5 cal kyr BP (e.g., Alley and others, 2005). Empirical (e.g., Fairbanks, 1989; Horton and others, 2005a) and modeling studies (e.g., Lambeck and others, 2002; Milne and others, 2005) suggest a significant reduction in eustatic contribution during the Holocene, beginning ca. 7 cal kyr ago.

Some of the best records of sea-level change in temperate areas have been derived from benthic intertidal foraminiferal assemblages contained in a range of post-glacial sedimentary deposits (e.g., Scott and Medioli, 1978; Gehrels, 1994). Transfer functions have subsequently been developed allowing precise reconstruction of former sea levels using a statistically based relationship between contemporary and fossil foraminiferal assemblages (e.g., Horton, 1999; Gehrels, 2000; Edwards and others, 2004; Patterson and others, 2004; Gehrels and others, 2005; Horton and Edwards, 2006; Boomer and Horton, 2006; Massey and others, 2006; Southall and others, 2006). In Australia, Horton and others (2003) and Woodroffe and others (2005) analyzed intertidal foraminiferal distributions to assess their ability to reconstruct former sea levels from mangrove environments from the Great Barrier Reef coastline (GBR). Furthermore, Cann and others (2002) used intertidal foraminifera as indicators of estuarine-lagoonal and oceanic influences in Holocene sediments of the Murray River, South Australia. A transfer function has been developed but never applied in mangrove environments of Northern Queensland, because of problems with foraminiferal preservation (Horton and others, 2003, 2005b; Woodroffe and others, 2005). Woodroffe and others (2005) and Berkeley and others (2006) demonstrate that foraminiferal preservation within mangrove sediments of the GBR coastline is problematic, concurring with the conclusions of Wang and Chappell (2001) and Debenay and others (2004), who conclude that foraminifera in mangrove environments are dramatically affected by taphonomic processes.

In this paper, we explore the utility of using subtidal rather than intertidal foraminifera to reconstruct former sea levels for tropical environments. We define subtidal as all environments from the innermost inner shelf to the middle shelf (0-100 m). Yokoyama and others (2000) inferred the timing of the Last Glacial Maxima from sea-level reconstructions for the Bonaparte Gulf, Western Australia, based on the classification of sedimentary facies using subtidal foraminifera. However, this classification was only semi-quantitative and had only four zones (open marine, shallow marine, marginal marine and brackish), giving limited water-depth constraints (Shennan and Milne, 2003; Peltier and Fairbanks, 2006). We present contemporary subtidal foraminiferal samples and associated environmental information from two embayments along the central GBR coastline to demonstrate the relationship of benthic foraminiferal assemblages with water depth. We generate a foraminiferal-based, subtidal transfer function to reconstruct former sea levels. These reconstructions are compared with regional geophysical models and published sea-level data.

STUDY AREA

Far-field locations such as Australia are particularly important locations for sea-level reconstructions because they enable the examination of the timing and abruptness of reduction in global melting during the Holocene and the effect of meltwater load on earth rheology. This enables a better understanding of the integrated melting history of global late Pleistocene ice sheets and the loading response of materials of the crust. In addition, sea-level variations that have occurred throughout the mid to late Holocene in far-field regions give an insight into natural variability within a climatic system that is similar to the present one. Sea-level research in Australia includes some of the earliest debates on hydro-isostasy (e.g., Clark and others, 1978) and, more recently, discussions regarding ocean loading and continental levering (e.g., Belperio and others, 1984; Baker and Haworth, 2000; Cann and others, 2002; Haworth and others, 2002; Sloss and others, 2005; Woodroffe, 2006). Larcombe and others (1995a) and Larcombe and Carter (1998) compiled an extensive database of Holocene sea-level observations for the GBR using supra-, inter- and subtidal indicators. The variability of the data caused a wide scatter of sea-level index points, with the result that it was only possible to generate an envelope of Holocene sea-level changes. Studies from the GBR region (e.g., Carter and others, 1993; Beaman and others, 1994; Larcombe and others, 1995a; Larcombe and Carter, 1998) have shown that the majority (> 70%) of existing sea-level data are subtidal in nature.

Cleveland Bay and Bowling Green Bay are embayments from the central GBR shelf region, Queensland, Australia (Fig. 1a). The GBR shelf is 100 km wide in the central region, with water depths reaching 80 m (Maxwell, 1968). The central region of the GBR is thought to have been tectonically stable since at least 13 cal kyr BP (Chappell and others, 1982, 1983). There is no evidence for local tectonic movements since 5.5 cal kyr BP, although Chappell and others (1982, 1983) suggested there might have been minor hydro-isostatic warping and subsidence normal to the coastline across the shelf since 6 cal kyr BP. Differential flexing along the inner shelf has probably been less than 1 m, similar to the magnitude of the mid-Holocene fall in relative sea level (Beaman and others, 1994). The apparent lack of tectonic movement in the central GBR indicates that the results of this study will be applicable to other sites in the region.

Cleveland Bay is a 325 km^2 embayment located on the east coast of north Queensland (Fig. 1b), immediately offshore of Townsville. The southern margin of the bay is formed by salt flats containing chenier ridges, where the muddy shoreline and tidal creeks entering into the bay are mangrove-fringed. The western edge of the bay, on the mainland, is backed by a flat, sandy coastal plain, which has been extensively modified by human activity over the last 100 years (removal of mangroves and sand dunes; McIntyre, 1996; Hardbattle, 2003). Separating Cleveland Bay from Halifax Bay to the west is Magnetic Island. The northern edge of Cleveland Bay is delineated arbitrarily by the 20 m isobath, which is also the outer edge of the inner shelf (Belperio, 1983; Carter and others, 1993), which is dominated by terrigenous sediments (Maxwell, 1968; Belperio, 1983; Johnson and others, 1986). The eastern edge of the bay is bound by a granite headland, which forms Cape Cleveland. Bowling Green Bay is the larger of the two embayments, around 600 km^2, and is located 30 km southeast of Cleveland Bay (Fig. 1c). The sand spit of Cape Bowling Green protects the eastern side of the bay from the prevailing southeasterly waves. In the south is a broad coastal plain containing tidal mudflats, mangrove creek systems and salt marshes. Driven by strong northward alongshore flows, Bowling Green Bay receives a significant proportion of the 3-20 Mt/y of suspended sediment supplied to the coast by the Burdekin River, which enters the lagoon immediately south of Cape Bowling Green (Belperio, 1979; Neil and others, 2002; Orpin and others, 2004). Within the Bowling Green Bay, the coastal plains are crossed by the Haughton River, which flows five to six months of the year and supplies sandy terrigenous sediment to the nearshore.

METHODOLOGY

Contemporary and fossil samples from Cleveland Bay and Bowling Green Bay were collected by researchers from James Cook University, Australia and the Australian Institute of Marine Science. The samples were collected on cruise numbers KG857, KG902, KG911 and KG912b aboard R/V *James Kirby*. We selected forty-three 10-cm^3 samples of surface sediment and ten vibracores from subtidal locations from transects within Cleveland Bay and Bowling Green Bay for foraminiferal and lithological analyses (Fig. 1). Details of the chronology and lithofacies of the vibracores have been published by Larcombe and others (1995a), McIntyre (1996) and Larcombe and Carter (1998). We selected one dated sample from each vibracore for foraminiferal analyses (Table 1). The lithology of all samples indicated they were analogous to the subtidal environments of Cleveland Bay and Bowling

Green Bay (Belperio, 1979, 1983; Carter and others, 1993; McIntyre, 1996; Larcombe and Carter, 1998; Orpin and others, 2004), thus improving the likelihood of reliable sea-level reconstructions. Furthermore, the selected radiocarbon-dates range from the early Holocene to present. We calibrated the radiocarbon data using OxCal (ver 3.10; Bronk Ramsey, 2005) and the marine04.14c dataset, where appropriate (Hughen and others, 2004). The resulting sequence of ages was used to constrain the variations in sea level identified from the subtidal foraminiferal data.

The water depths of the contemporary and fossil samples were calculated from depth soundings taken at sampling points, taken with a 3.5 kHz precision depth recorder (using, in general, a 0.25 s firing rate, 6 kHz bandwidth and 0.5 ms pulse length). These readings were corrected for the depth of the transducer below the sea surface, then converted to Australian Height Datum (AHD) through using the date and time of sample collection and tide gauge records at Townsville. The resulting magnitude of the errors is between ± 0.3 m and ± 0.5 m (Hardbattle, 2003). Contemporary and fossil foraminiferal-sample preparation followed Scott and others (2001). Samples were wet-sieved through sieves with 500-μm and 63-μm openings and decanted using a wet splitter (Scott and Hermelin, 1993). We examined the >500 μm and decanted fractions before discarding them. We did not use any floatation techniques, and all the samples were picked wet. We analyzed the total assemblage. Modern and fossil samples produced foraminiferal counts >250 individuals per sample. The species were identified with reference to a number of publications, namely Brady (1884), Brönnimann and Whittaker (1993), Jones (1994), Loeblich and Tappan (1994), Yassini and Jones (1995) and Hayward and others (1997, 1999), and by study of reference collections in the Natural History Museum, London (Plate 1).

We used two multivariate methods to detect, describe and classify patterns within the contemporary foraminiferal dataset. Unconstrained cluster analysis, based on the unweighted Euclidean distance with no transformation or standardization of the percentage data and amalgamation using the incremental sum of squares within each group (Grimm, 2004), was used to classify contemporary samples into more-or-less homogeneous faunal zones (clusters). We used unconstrained cluster analysis because it compares samples without any stratigraphic constraint. Detrended correspondence analysis (DCA), an ordination technique, was used to represent samples as points in multi-dimensional space, where similar samples plot close together and dissimilar samples apart (ter Braak and Smilauer, 1997-2003). Thus, cluster analysis is effective in classifying the samples according to their foraminiferal assemblage. DCA gives further information about the pattern of variation within and between groups, which is important because the precise boundaries between clusters can be arbitrary (Birks, 1986, 1992). Thus, our selection of foraminiferal zones was based on whether the samples within each cluster were mutually exclusive in ordination space. The water depth of each station within the clusters determined the bathymetric distribution of each delineated subtidal environment.

We determined the grain size distribution using a Beckman Coulter laser particle-size analyzer, following the sediment preparation procedures of Goff and others (2004) and Hawkes and others (in press). Organic content of the sediments was determined by loss on ignition (LOI), following the procedures of Ball (1964).

RESULTS

CLEVELAND BAY

The two transects in Cleveland Bay were 8 km and 4 km in length and covered water depths from -4.2 m to -9.8 m AHD. The Cleveland Bay seabed was a silty sand with low organic content (<5%). The sand content increased seaward from 44% at a water depth of -5.6 m AHD to 98% at -7.4 m AHD. We identified twenty-six foraminiferal species from the eighteen sampling stations of the two transects at Cleveland Bay. The assemblages of the two transects were dominated by five species (*Elphidium hispidulum, Pararotalia venusta, Planispirinella exigua, Quinqueloculina venusta* and *Triloculina oblonga*; Fig. 2). The landward section of Transect 1 was dominated by *E. hispidulum,* with notable contributions from *T. oblonga.* The maximum relative abundance of both these species (30% and 12%, respectively) occurred at 2.9 km along the transect, with a water depth of -5.5 m AHD.

These species were replaced by *Q. venusta and P. exigua* at deeper water depths. The maximum relative abundance of *Q. venusta* (16%) occurred at 6 km along the transect in a water depth of -6.0 m AHD, whereas *P. exigua* peaked (24%) at the seaward end of the transect, with a water depth of -9.8 m AHD.

The landward edge of Transect 2 was dominated by *E. hispidulum* and *P. venusta.* Their maximum relative abundances (23% and 24%, respectively) occurred at a water depth of -4.2 m AHD. These species were replaced by *Q. venusta* and *P. exigua*. The relative abundance of *Q. venusta* exceeded 30% at 2.2 km along the transect, with a water depth of -7.9 m AHD. The seaward edge of the transect had the maximum relative abundance of *Q. pseudoreticulata* (17% at a water depth of -6.0 m AHD).

Multivariate analyses of a combined dataset of transects 1 and 2 identified two foraminiferal zones (Fig. 3). Zone CB-I was dominated by *Amphistegina lessonii, P. venusta*, *Q. venusta* and *Q. pseudoreticulata*. This zone had a water depth range of -4.2 m to -7.9 m AHD. Zone CB-II was occupied by *E. hispidulum, H. depressula* and *P. exigua*, the latter of which exceeded 10% in all samples. This zone had a water depth range of -5.5 m to -9.8 m AHD.

Bowling Green Bay

The Bowling Green Bay transect was much longer (65 km) than that of the Cleveland Bay and extended from a depth of -6.7 m AHD through the inner and middle shelves of the GBR lagoon to a depth of -48.0 m AHD. The substrate of the Bowling Green Bay transect was a silty sand, with a low clay (≤ 13%) and organic (< 8%) content. The percentage of silt decreased with increasing water depth from 22% at -10.1 m AHD to 4.2% at -48.0 m AHD. We identified thirty-one species from twenty-five stations along the Bowling Green Bay transect. The assemblage was dominated by five species (Fig. 4). *Elphidium hispidulum, Planispirinella exigua* and *Quinqueloculina venusta* dominated the inner shelf. Indeed, all species had their maximum abundances within the inner shelf; *E. hispidulum*

(19%), *P. exigua* (16%) and *Q. venusta* (17%) peaked at 4.5 km, 10 km and 4.5 km along the transect, respectively, within shallow water depths (>-13 m AHD). The proportion of these three species decreased at the transition with the middle shelf, to be replaced by *Amphistegina lessonii* and *Dendritina striata*. High relative abundances of *D. striata* were restricted to the landward section of the middle shelf, with its maximum abundance (23%) occurring at 27.5 km along the transect, with a water depth of -25 m AHD. *A. lessonii* dominated the seaward section of the middle shelf with a maximum abundance of 41% at 52 km along the transect with a water depth of -38.5 m AHD. Multivariate analysis clearly identified two zones (Fig. 5). Zone BGB-I comprised 12 sites and was dominated by *E. hispidulum, P. exigua* and *Q. venusta*, with a virtual absence of *A. lessonii, D. striata* and *Operculina complanata*. The zone occurred at water depths of -6.7 m to -17.0 m AHD. In contrast, Zone BGB-II encompassed 13 sites where *A. lessonii, D. striata* and *O. complanata* were dominant. The relative abundance of *A. lessonii* exceeded 20% in 10 of the 13 samples. The zone included water depths from -18.5 to -48.0 m AHD.

TRANSFER FUNCTION DEVELOPMENT

We combined the subtidal foraminifera from Cleveland Bay and Bowling Green Bay into one modern dataset to increase the range of environments to ensure that most fossil samples have a modern analogue. This will introduce inherent “noise” into the data set because Cleveland Bay and Bowling Green Bay have different physiographic conditions. Nevertheless, DCA of the combined dataset showed considerable overlap between sites (Fig. 6). We developed a transfer function using a unimodal-based technique known as weighted averaging partial least squares (WA-PLS; Juggins, 2004). The dataset consisted of thirty-one species and forty-three samples. We did not screen any samples or species from the dataset. The WA-PLS transfer function produced results for five components. The choice of component depended upon the prediction statistics: root-mean square of the error of prediction (RMSEP) and the squared correlation (r^2) of observed versus predicted values.

The RMSEP indicates the systematic differences in prediction errors, whereas the r^2 measures the strength of the relationship of observed versus predicted values. These statistics were calculated as "apparent" measures in which the whole, contemporary dataset was used to generate the transfer function and assess the predictive ability. The data were also jack-knifed (also known as "leave-one-out" measures; Birks, 1995) to produce a measure of the overall predictive abilities of the dataset. Jack-knifing is the simplest approach of cross-validation (ter Braak and Juggins, 1993) where the reconstruction procedure is applied *n* times using a modern dataset of size (*n* – 1). In each of the *n* predictions, one sample is left out in turn, and the calibration function based on the (*n* – 1) sites in the modern dataset is applied to the omitted sample, giving a predicted water depth, which can be subtracted from the observed water depth to produce a prediction error for the sample (Birks, 1995). We chose component two for the transfer function because it performed significantly better than component one when jack-knifed errors were considered; prediction errors (RMSEP) were lower, and squared correlations (r^2) were higher (Table 2). Using component two, the relationship between observed and subtidal foraminiferal-predicted elevation was very strong (Fig. 7), a result that illustrated the robust performance of the WA-PLS transfer function (r^2_{jack} = 0.90). These results indicated that reconstructions of former sea levels are possible ($RMSEP_{jack}$ = 3.50 m).

DISCUSSION

SUBTIDAL FORAMINIFERAL DISTRIBUTION

Our multivariate analysis of the subtidal foraminifera of Cleveland Bay and Bowling Green Bay has identified two foraminiferal zones. The first zone is dominated by *Elphidium hispidulum, Pararotalia venusta, Planispirinella exigua, Quinqueloculina venusta* and *Triloculina oblonga* and occupied the shallow-water, inner-shelf environment. Similar subtidal assemblages have been found elsewhere in tropical and temperate environments. For example, *E. hispidulum* has been found in coral-enclosed lagoons, bays and outer reef slopes from the western Pacific (Loeblich and Tappan, 1994; Hayward and others, 1997), New South Wales and Queensland (Albani and Yassini, 1993) and New Caledonia (Debenay, 1988). *P. venusta* occurs in the sedimentary facies of Exmouth Gulf, northwestern Australia (Orpin and others, 1999a) and Madang Reef and Lagoon, Papua New Guinea (Langer and Lipps, 2004). *T. oblonga* has been found in normal-marine to hypersaline salt marshes and lagoonal environments of Georgia and Texas, USA, Bermuda, Tobago and French Guiana, in water depths less than 10 m (e.g., Phleger, 1960; Brasier, 1975; Radford, 1976; Goldstein and Frey, 1986; Murray, 1991; Debenay and others, 2001).

The second zone, dominated by *Amphistegina lessonii, Dendritina striata* and *Operculina complanata*, occurred in the middle shelf. This area is between the shore-connected sediment wedge and the inner edge of the main reef tract at approximately 40 m. A study of the Gulf of Elat, in the Red Sea, suggested that *A. lessonii* has a depth range to approximately 90 m below sea level (Hottinger, 1977). Indeed, Hottinger (1977) found the maximum abundance of this species at depths of 35-40 m, similar to our findings along the Bowling Green Bay transect. Murray (1991) described two *A. lessonii* associations: firstly, a continental shelf association from Seto, Japan and the Banda Sea, with a sandy substrate and water depths of 0-10 m (Uchio, 1962, 1967; van Marle, 1988); and secondly, beach and lagoon associations from numerous tropical islands of the Pacific, with water depths of 0 m to 38 m (Hallock, 1984; Debenay, 1985). *O. complanata* occurred preferentially in sandy substrates and low light intensities (Hohenegger and others, 2000). This species has been found in Bali, Indonesia and Japan (Renema, 2002; Renema and Troelstra, 2001; Renema and others, 2001; Hohenegger and others, 2000). Hughes (1977) identified *O. complanata* from the Solomon Islands at depths of 30 m to 48 m. Renema (2006) also identified *D. striata* within the carbonate shelf facies of a barrier reef system in the Berau area, east Kalimantan, Indonesia.

THE RELATIONSHIP WITH WATER DEPTH

In 1933, Natland showed that the distribution of shelf foraminifera off California could be related to depth below sea level (Natland, 1933). Bandy and co-workers (e.g., Bandy and Chierici, 1966) later suggested that certain species always occupy the same depth interval (isobathyal species). However, depth is simply a factor, along with latitude and longitude, in locating a sample in three-dimensional space (Buzas, 1974); the biotic and abiotic environmental factors that control the distribution of foraminifera vary with depth (for reviews see Boltovskoy and Wright, 1976; Sen Gupta, 1977, 1982; Murray, 1991; Hayward and others, 1999, 2006; Morigi and others, 2005). Therefore, the depth distribution of foraminiferal species varies from basin to basin (e.g., Culver and Buzas, 1980, 1981) but, even so, depth relatable patterns are well developed and relatively easily recognized. Hayward and others (1999) noted that depth zonations at inner to mid shelf depths are finer (accuracy of ca. 10-20 m) than those of outer shelf and upper bathyal (accuracy of ca. 150 to 200 m) and mid bathyal or deeper depths (accuracy of ca. 200-1000 m), but statistical approaches (e.g., Culver, 1988) can be used to delineate finer zonation schemes. Our data indicate that the distributional patterns of the subtidal foraminifera of this study can be related to water depth (Fig. 8). *Amphistegina lessonii* and *Operculina complanata* showed strong positive correlations with water depth, whereas *Elphidium hispidulum, Pararotalia venusta, Planispirinella exigua* and *Quinqueloculina venusta* showed strong negative relationships with water depth; indeed the correlation coefficients (*r*) exceed the critical value at $p = 0.01$. *Dendritina striata* illustrated a unimodal relationship with water depth.

RECONSTRUCTION OF FORMER SEA LEVELS

We calibrated the subtidal regional transfer function to ten radiocarbon-dated samples from vibracores of Cleveland Bay (Fig. 1d,). The transfer function assigned a water depth to each sample (Table 1). We used bootstrapping to derive a sample-specific root mean squared error of prediction for individual samples (Birks and others, 1990; Line and others, 1994). Errors are likely to be relatively small for fossil assemblages consisting of taxa that are frequent and abundant in the modern dataset and to be relatively large for fossil assemblages consisting of taxa that are infrequent and rare in the modern dataset (Birks, 1995). We also employed the modern analogue technique (Juggins, 2004) to evaluating the likely reliability of water depth reconstructions based on the subtidal transfer function. The technique compares numerically, using chi-square distance dissimilarity coefficient, the foraminiferal assemblage in a fossil sample with the foraminiferal assemblages in all available modern samples. Through using the largest minimum dissimilarity coefficient (Woodrofffe, 2006), we illustrated that all fossil samples had a "good" analogue in the modern dataset. Foraminiferal assemblages of the radiocarbon-dated samples showed a group of species comparable to the contemporary environment (Fig. 9). The lowest sample sum of contemporary foraminifera in a fossil assemblage was 75%. Samples 911v15, 911v16 and 911v11 were dominated by *Amphistegina lessonii* with contributions from *Dendritina striata, Operculina complanata* and *Pararotalia venusta,* all of which are indicative of middle shelf environments. The reconstructed water depths were the deepest of all radiocarbon-dated samples (<-27 m AHD). In contrast, samples 911v18, 902v113 and 902v106 had the shallowest assigned water depth (>-9 m AHD). *Elphidium albanii* was the most dominant species in these samples and occurred in the modern inner shelf environment of Bowling Green Bay and Cleveland Bay. The sample-specific errors for the water depth reconstructions varied between ± 3.7 m and ± 4.5 m. These errors are relatively small when compared to the long environmental gradient of the dataset (-4.2 m AHD to -48.0 m AHD); the sample-specific errors are at most 12% of the vertical range of the dataset. In comparison, some of the smallest sample-specific errors (± 0.05 m to ± 0.21 m) were from salt marshes in North Carolina, USA (Horton and others, 2006), however these represented 14% of the vertical range of the modern dataset. Furthermore, the errors are comparable to reconstructions based on corals, which are by far the most widely used sea-level indicators in tropical locations (Fairbanks, 1989; Toscano and Macintyre, 2003; Peltier and Fairbanks, 2006).

In addition to the sample-specific errors, caution should be exercised when using transfer functions, because characteristics within the contemporary and fossil data may affect the accuracy of water depth reconstructions. There is an uneven spatial sampling within the contemporary data with respect to water depth. Twenty of the forty-three samples were taken in water depths of -4 m to -10 m AHD. The transfer function reconstructions are made from individual water depth measurements for each dated sample rather than samples in sequences that could reveal deepening or shallowing trends. Thus, the reconstruction may be erroneous because of post-depositional changes, particularly poor preservation of the calcareous tests, bioturbation and transport of tests from and into an assemblage. The loss of calcareous tests is an important taphonomic effect experienced by benthic foraminifera, occurring mainly in regions of high organic carbon concentrations (e.g., Murray and Alve, 1999). The organic content of Bowling Green Bay and Cleveland Bay, however, was less than 8%, suggesting the dissolution of calcareous tests is minimal. Bioturbation commonly occurs in the top few centimeters of sediments below the sea floor with slower, more episodic, bioturbation below this depth. However, bioturbation can occur at depths greater than 12 cm (Aller and Cochran, 1976). The rate varies seasonally and is highest in summer (Green and others, 1993). Bioturbation is critical in promoting the dissolution of calcareous foraminiferal tests as it prevents reaction product build-up and stimulates aerobic metabolites, iron sulfide oxidation and nitrification (Green and others, 1993). Conversely, it can result in foraminifera bypassing the dissolution zone either through biogenic subduction or by falling into tubes or burrows (Green and others, 1993). Regarding the transport of foraminifera, the headlands of Cape Bowling Green and Cape Cleveland protect the embayments from the dominant southeast waves and alongshore currents, which, in the long-term, transport sediments and foraminiferal tests regionally to the northwest. However, the western side of Bowling Green Bay is much more exposed than in the lee of the headland (e.g., Belperio, 1983).Thus, much of the sediment is resuspended (McIntyre, 1996; Larcombe and Carter, 2004), which may mix the foraminifera. Furthermore, the embayments lie open to northerly and northeasterly weather, and the effects of tropical cyclones, which are a common seasonal feature of the GBR shelf, typically occurring two to three times per summer at this latitude (Oliver, 1978; Gagan and others, 1988, 1990; Massell and Done, 1993; Larcombe and Carter, 2004). Despite these processes, our samples lack abraded, etched or broken tests and consist of the full spectrum of test sizes. This is likely to be partly related to the time elapsed since the last major cyclone-driven flows along the middle shelf (Larcombe and Carter, 2004). Unfortunately, there are no direct methods of detecting erroneous reconstructed reference water depths. Therefore, the most important indirect method is comparison with other lithostratigraphical, biostratigraphical and modeling techniques.

To further examine the reliability of the transfer function approach, we have compared our sea-level reconstructions with existing geophysical model and published sea-level data from the study area. Figure 10 shows two sea-level predictions for the GBR coastline based on a compressible Maxwell visco-elastic Earth model, which is spherically symmetric and self-gravitating (Horton and others, 2005a; Milne and others, 2005). The elastic and density structure of the model are taken from seismic constraints (Dziewonski and Anderson, 1981). The viscous structure is defined in three layers: a very high viscosity outer shell, or lithosphere, with thicknesses of 96 and 120 km; a sub-lithosphere upper mantle region with a viscosity of 5×10^{20} Pas to a depth of 670 km; and a lower mantle region with a viscosity of 10^{22} Pas from 670 km to the core-mantle boundary. This viscosity structure is broadly compatible with that inferred in a number of recent studies (e.g., Mitrovica and Forte, 1997; Kaufmann and Lambeck, 2003; Milne and others, 2005). The ice model adopted to generate the predictions shown in Figure 10 is based on the ICE-3G deglaciation history (Tushingham and Peltier, 1991). A number of revisions have been made to the original ICE-3G model. The most significant changes are the addition of a glaciation phase and an increase in the volume and melt chronology of the Laurentide component of the model in order to produce a good fit to the Barbados sea-level record, based on assuming the reference viscosity model described above. The ice model is characterized by a large decrease in the rate of melt at 7 cal. kyr BP, so the sea-level predictions display a marked highstand at this time (see Milne and others, 2005 for more details).

Sea-level index points were extracted from the transfer-function output by combining the water-depth reconstructions with the elevation of each sediment sample relative to AHD. These index points were then placed in a temporal framework using the chronological data (Table 1). The general pattern of relative sea-level change indicated by the subtidal transfer function is consistent with the results of geophysical modeling (Fig. 9). Furthermore, in common with other far-field regions, the general pattern of relative sea-level change is of an initially rapid rise during the early Holocene, from -8.9 ± 4.5 m AHD at 9.3-8.6 cal kyr BP. This rise culminated in a middle Holocene highstand of ca. +1.7 ± 3.9 m AHD between 7.6-6.4 cal kyr BP, and then a fall to the present. Chappell and others (1983) and Beaman and others (1994) inferred that relative sea level rose rapidly through the early Holocene, rising above the present level at ca. 6.7 cal kyr BP; the amplitude of the highstand was, however, greater than in this study. Larcombe and others (1995a) and Larcombe and Carter (1998) concluded that the Holocene sea-level highstand occurred slightly later at ca. 6.3 cal kyr BP, but with a near identical amplitude to the current study (ca. 1.5 m above the present level). Beaman and others (1994) used the elevations of intertidal rock oyster shells on Magnetic Island to suggest that the mid-Holocene highstand was ca. +1.7 m AHD between 6.5-4.4 cal kyr BP. An interpolation of Chappell and others' (1982) isobase map predicts that relative sea level was 1-2 m above the present level in Cleveland Bay at 6.3 cal kyr BP.

This paper indicates that sea-level reconstructions using subtidal foraminiferal-based transfer functions can produce reliable results. However, the Holocene physiography and environmental history of this relatively wide central section of the GBR shelf may be favorable to the success of this technique; it should not be assumed that this technique might be reproducible elsewhere. Specifically, prior to and during the mid-Holocene highstand, the along-contour, sediment-transport on the GBR shelf (Larcombe and Woolfe, 1999; Gagan and others, 1988, 1990; Larcombe and Carter, 2004) and the resulting strong regional cross-shelf sedimentary gradients (Maxwell, 1968; Belperio, 1983, 1988; Johnson and Searle, 1984; Scoffin and Tudhope, 1985; Carter and others, 1993) appear conducive to producing a cross-shelf zonation in sedimentary environments, and, by implication, in foraminiferal communities. Furthermore, from the highstand to the present-day, the along-shelf nature of currents and sediment transport (Wolanski, 1994; Larcombe and others, 1995b; Orpin and others, 1999b; Larcombe and Carter, 2004) and the heterogeneity of the relatively sheltered embayments (Belperio

1983, 1988; Carter and others, 1993; McIntyre, 1996) are important factors in producing a strong zonation in the modern sediments. The three-dimensional nature of the currents and the sediment transport, during the highstand and since then, appears highly favorable to the success of this technique.

SUMMARY

Intertidal foraminifera have been used to reconstruct Holocene sea-level changes from coastlines around the world. In this paper, we assessed the utility of subtidal benthic foraminifera for sea-level reconstructions for the Central GBR. We collected contemporary foraminiferal samples from Cleveland Bay and Bowling Green Bay. The water depths of these samples ranged from -4.2 m to -48.0 m AHD. Multivariate analysis of the subtidal foraminifera identified two foraminiferal zones: an inner shelf zone occupied by *Elphidium hispidulum, Pararotalia venusta, Planispirinella exigua, Quinqueloculina venusta* and *Triloculina oblonga*; and a middle shelf zone dominated by *Amphistegina lessonii, Dendritina striata* and *Operculina complanata*. The zonations of the study areas and relative abundances of individual species suggested that the distribution of subtidal foraminifera is related to water depth.

These contemporary subtidal foraminiferal data were used to develop a predictive transfer function capable of inferring the past water depth of a sediment sample from its foraminiferal content. The results indicated a robust performance of the transfer function (r^2_{jack} = 0.90), with errors comparable with coral-based reconstructions ($RMSEP_{jack}$ = 3.50 m). Caution should be exercised, however, since characteristics within the foraminiferal data may affect the accuracy of water depth reconstructions, in particular transport of tests from and into an assemblage. Using the transfer function, we produced ten sea-level index points, which revealed an upward trend of Holocene relative sea level from a minimum of -8.9 ± 4.5 m AHD at 9.3-8.6 cal kyr BP to a mid-Holocene highstand of ca. +1.7 ± 3.9 m AHD at 7.6-6.4 cal kyr BP.

ACKNOWLEDGMENTS

We gratefully acknowledge the advice, comments and general encouragement given by Bob Carter. We are indebted to James Cook University and AIMS for access to modern and fossil samples. We thank the Design and Imaging Unit of the Department of Geography, University of Durham, UK for the production of the figures. The paper is a contribution to IGCP Project 495 "Quaternary Land-Ocean Interactions: Driving Mechanisms and Coastal Responses."

REFERENCES

ALBANI, A. D., and YASSINI, I., 1993, Taxonomy and distribution of the family Elphidiidae (Foraminiferida) from shallow Australian waters: University of New South Wales Centre for Marine Science, Technical Contribution No. 5, 51 p.

ALLER, R. C., and COCHRAN, J. K., 1976, ^{234}Th: ^{238}U disequilibrium in nearshore sediment: particle reworking and diagenic time scales: Earth Planetary Science Letters, v. 20, p. 37-50.

ALLEY, R. B., CLARK, P. U., HUYBRECHTS, P., and JOUGHIN, I., 2005, Ice-sheet and sea-level changes: Science, v. 310, p. 456-460.

BAKER, R. G. V., and HAWORTH, R. J., 2000, Smooth or oscillating late Holocene sea-level curve? Evidence from the palaeo-zoology of fixed biological indicators in east Australia and beyond: Marine Geology, v. 163, p. 367-386.

BALL, D. F., 1964. Loss-on-ignition as an estimate of organic matter and organic carbon in non-calcareous soils: Journal of Soil Science, v. 15, p. 84-92.

BANDY, O. L., and CHIERICI, M. A., 1966, Depth-temperature evaluation of selected California and Mediterranean bathyal foraminifera: Marine Geology, v. 4, p. 259-271.

BARD, E., HAMELIN, B., ARNOLD, M., MONTAGGIONI, L., CABIOCH, G., FAURE, G., and ROUGERIE, F., 1996, Deglacial sea-level record from Tahaiti corals and the timing of global meltwater discharge: Nature, v. 382, p. 241-244.

BEAMAN, R., LARCOMBE, P., and CARTER, R. M., 1994, New evidence for the Holocene sea-level high from the inner shelf, Central Great Barrier Reef, Australia: Journal of Sedimentary Research, v. 64, p. 881-885.

BELPERIO, A.P., 1979, The combined use of wash load and the bed material load rating curves for the calculation of total load: An example from the Burdekin River, Australia: Catena, v. 6, p. 317-329.

———, 1983, Terrigenous sedimentation in the central Great Barrier Reef lagoon: a model from the Burdekin region: Bureau of Mineral Resources, Journal of Australian Geology and Geophysics, v. 8, p. 179-190.

———, 1988, Terrigenous and carbonate sedimentation in the GBR province, *in* Doyle, L. J., and Roberts, H. H. (eds.), Carbonate-Clastic Transitions: Developments in Sedimentology, v. 42: Elsevier, Amsterdam, p. 143–174.

———, Hails, J. R., Gostin, V. A., and Polach, H. A., 1984, The stratigraphy of coastal carbonate banks and Holocene sea levels of northern Spencer Gulf, South Australia: Marine Geology, v. 61, p. 297-313.

Berkeley, A., Perry, C. T., Smithers, S., and Horton, B. P., 2006, Preservation of foraminifera in tropical intertidal environments: implications for palaeoenvironmental studies: European Geosciences Union General Assembly, Vienna, 02-07 April 2006, Geophysical Research Abstracts, v. 8, 02140.

Birks, H. J. B., 1986, Numerical zonation, comparison and correlation of Quaternary pollen-stratigraphical data, *in* Berglund, B. E. (ed.), Handbook of Holocene Palaeoecology and Palaeohydrology: John Wiley and Sons Ltd, London, p. 743-773.

———, 1992, Some reflections on the application of numerical methods in Quaternary palaeoecology: University of Joensuu Publication, Karelian Institute, Joensuu, Finland, v. 102, p. 7-20.

———, 1995, Quantitative palaeoenvironmental reconstructions, *in* Maddy, D., and Brew, J. S. (eds.), Statistical Modeling of Quaternary Science Data: Technical Guide No. 5: Quaternary Research Association, Cambridge, p.161-254.

———, Line, J. M., Juggins, S., Stevenson, A. C., and ter Braak, C. J. F., 1990, Diatom and pH reconstruction: Philosophical Transactions of the Royal Society of London, v. 327, p. 263-278.

Boltovskoy, E., and Wright, R., 1976, Recent Foraminifera: Dr. W. Junk, Publishers, The Hague, 515 p.

BOOMER, I., and HORTON, B. P., 2006, Holocene relative sea-level movements along the North Norfolk Coast, UK: Palaeogeography, Palaeoclimatology, Palaeoecology, v. 23, p. 32-51.

TER BRAAK, C., and SMILAUER, P., 1997-2003, Canoco for Windows, Version 4.51.

BRASIER, M. D., 1975, Ecology of Recent sediment-dwelling and phytal foraminifera from the lagoons of Barbuda, West Indies: Journal of Foraminiferal Research, v. 5, p. 42-62.

BRONK RAMSEY, C., 2005, OxCal Program v3.10, Oxford Radiocarbon Accelerator Unit, Research Lab for Archaeology, University of Oxford, Oxford, UK, http://c14.arch.ox.ac.uk/oxcal.html.

BRÖNNIMANN, P., and WHITTAKER, J. E., 1993, Taxonomic revision of some recent agglutinated foraminifera from the Malay Archipelago in the Millett Collection, Natural History Museum, London: Bulletin of the Natural History Musuem London, v. 59, p. 107–124.

BRADY, H. B., 1884, Report on the foraminifera dredged by H.M.S. Challenger during the years 1873-1876, *in* Reports of the Scientific Results of the Voyage of the H.M.S. Challenger, Zoology, London, v. 9, 814 p.

BUZAS, M. A., 1974, Review: Journal of Foraminiferal Research, v. 4, p. 224.

CANN, J. H., HARVEY, N., BARNETT, E. J., BELPERIO, A. P., and BOURMAN, R. P., 2002, Foraminiferal biofacies eco-succession and Holocene sea levels, Port Pirie, South Australia: Marine Micropaleontology, v. 44, p. 31-55.

CARTER, R. M., JOHNSON, D. P., and HOOPER, K. G., 1993, Episodic post- glacial sea-level rise and the sedimentary evolution of a tropical embayment (Cleveland Bay, Great Barrier Reef shelf, Australia): Australian Journal of Earth Science, v. 40, p. 229- 255.

CHAPPELL, J., and POLACH, H., 1991, Post-glacial sea level rise from a coral record at Huon Peninsula, Papua New Guinea: Nature, v. 349, p. 147-149.

———, RHODES, E. G., THOM, B. G., and WALLENSKY, E., 1982, Hydro-isostasy and the sea-level isobase of 5500 BP in north Queensland, Australia: Marine Geology, v. 49, p. 81-90.

———, CHIVAS, A., WALLENSKY, E., POLACH, H. A., and AHARON, P., 1983, Holocene palaeo-environmental changes, central to north Great Barrier Reef inner zone: BMR Journal of Australian Geology and Geophysics, v. 8, p. 223-235.

CLARK, J. A., FARRELL, W. E, and PELTIER, W. R., 1978, Global changes in post glacial sea level: a numerical calculation: Quaternary Research, v. 9, p. 265-287.

CULVER, S. J., 1988, New foraminiferal depth zonation in the northwestern Gulf of Mexico: Palaios, v. 3, p. 69-85.

———, and BUZAS, M. A., 1980, Distribution of Recent benthic foraminifera off the North American Atlantic coast: Smithsonian Contributions to the Marine Sciences, no. 6, 512 p.

———, and ———, 1981, Distribution of Recent benthic foraminifera in the Gulf of Mexico. Smithsonian Contributions to the Marine Sciences, no. 8, 898 p.

DEBENAY, J. P., 1985, Le genre *Amphistegina* dans le lagon de Nouvelle-Calédonie (S.W. Pacifique): Revue de Micropaléontologie, v. 28, p. 167-180.

———, 1988, Foraminifera larger than 0.5 mm in the southwestern lagoon of New Caledonia: distribution related to abiotic properties: Journal of Foraminiferal Research, v. 18, p. 158-175.

———, GUIRAL, D., and PARRA, M., 2004, Behaviour and taphonomic loss in foraminiferal assemblages of mangrove swamps of French Guiana: Marine Geology, v. 208, p. 295-314.

———, GESLIN, E., EICHLER, B. B., DULEBA, W., SYLVESTRE, F., and EICHLER, P., 2001, Foraminiferal assemblages in a hypersaline lagoon, Aruruama (R.J.) Brazil: Journal of Foraminiferal Research, v. 31, p. 133-151.

DZIEWONSKI, A. M., and ANDERSON, D. L., 1981, Preliminary Reference Earth Model (PREM): Physics of the Earth and Planetary Interiors, v. 25, p. 297-356.

EDWARDS, R. J., VAN DE PLASSCHE, O., GEHRELS, W. R., and WRIGHT, A. J., 2004, Assessing sea-level data from Connecticut, USA, using a foraminiferal transfer function for tide level: Marine Micropaleontology, v. 51, p. 239-255.

FAIRBANKS, R. G., 1989, A 17,000-year glacio-eustatic sea level record: influence of glacial melting rates on the Younger Dryas event and deep-ocean circulation: Nature, v. 342, p. 637-642.

GAGAN, M. K., CHIVAS, A. R., and HERCZEG, A. L., 1990, Shelf-wide erosion, deposition, and suspended sediment transport during cyclone Winifred, Central Great Barrier Reef, Australia: Journal of Sedimentary Petrology, v. 60, p. 456-470.

———, JOHNSON, D. P., and CARTER, R. M., 1988, The cyclone Winifred strom bed, central Great Barrier Reef shelf Australia: Journal of Sedimentary Petrology, v. 58, p. 845-856.

GEHRELS, W. R., 1994, Determining relative sea-level change from saltmarsh foraminifera and plant zones on the coast of Maine, USA: Journal of Coastal Research, v. 10, p. 990-1009.

———, 2000, Using foraminiferal transfer functions to produce high-resolution sea-level records from salt-marsh deposits, Maine, USA: The Holocene, v. 10, p. 367-376.

———, KIRBY, J. R., PROKOPH, A., NEWNHAM, R. M., ACHTERBERG, E. P., EVANS, E. H., BLACK, S., and SCOTT, D. B., 2005, Onset of recent rapid sea-level rise in the western Atlantic Ocean: Quaternary Science Reviews, v. 24, p. 2083-2100.

GOFF, J., MCFADGEN, B. G., and CHAGUÉ-GOFF, C., 2004, Sedimentary differences between the 2002 Easter storm and the 15th-century Okoropungo tsunami, southeastern North Island, New Zealand: Marine Geology, v. 204, p. 235-250.

GOLDSTEIN, S. T., and FREY, R. W., 1986, Salt marsh foraminifera, Sapelo Island, Georgia: Senckenbergiana Maritima, v. 18, p. 97-121.

GREEN, M. A., ALLER, R. C. and ALLER, J. Y., 1993, Carbonate dissolution and temporal abundances of foraminifera in Long Island Sound sediments: Limnology and Oceanography, v. 38, p. 331-345.

GRIMM, E. C., 2004, Tilia View: version 2.0.2. Research and Collections Center, Illinois State Museum.

HALLOCK, P., 1984, Distribution of selected species of living algal symbiont-bearing foraminifera on two Pacific coral reefs: Journal of Foraminiferal Research, v. 14, p. 250-261.

HARDBATTLE, M. I. J., 2003, Holocene Relative Sea-Level Reconstruction for the Central Great Barrier Reef, Australia: A Subtidal Foraminiferal Approach. Unpublished Masters Thesis, University of Durham, Durham, UK, 109 p.

HAWKES, A. D., BIRD, M., COWIE, S., GRUNDY-WARR, C., HORTON, B. P., TAN SHAU HWAI, A., LAW, L., MACGREGOR, C., NOTT, J., EONG ONG, J., RIGG, J., ROBINSON, R., TAN-MULLINS, M., TIONG SA, T., and ZULFIGAR, Y., in press, The sediments deposited by the 2004 Indian Ocean tsunami along the Malaysia-Thailand Peninsula: Marine Geology.

HAWORTH, R. J., BAKER, R. G. V., and FLOOD, P. G., 2002, Predicted and observed Holocene sea-levels on the Australian coast: what do they indicate about hydro-isostatic models in far-field sites?: Journal of Quaternary Science, v. 17, p. 581-591.

HAYWARD, B. W., HOLLIS, C. J. and GRENFELL, H. R., 1997, Recent Elphidiidae (Foraminiferida) of the South-west Pacific and fossil Elphidiidae of New Zealand: New Zealand Geological Survey Paleontological Bulletin, v. 72, 166 p.

———, GRENFELL, H. R., REID, C. M., and HAYWARD, K. A., 1999, Recent New Zealand shallow-water benthic foraminifera: taxonomy, ecologic distribution, biogeography, and use in paleoenvironmental assessment: Institute of Geological and Nuclear Sciences Monograph, v. 21, 258 p.

———, ———, SABAA, A. T., HAYWARD, C. M., and NEIL, H., 2006, Ecologic distribution of benthic foraminifera, offshore northeast New Zealand: Journal of Foraminiferal Research, v. 36, p. 332-354.

HOHENEGGER, J., YORDANOVA, E., and HATTA, A., 2000, Remarks on west Pacific Nummulitidae (Foraminifera): Journal of Foraminiferal Research, v. 30, p. 3-28.

HORTON, B. P., 1999, The contemporary distribution of intertidal foraminifera of Cowpen Marsh, Tees Estuary, UK: implications for studies of Holocene sea-level changes: Palaeogeography, Palaeoclimatology, Palaeoecology, Special Issue, v. 149, p. 127-149.

———, and EDWARDS, R. J., 2006, Quantifying Holocene Sea Level Change Using Intertidal Foraminifera: Lessons from the British Isles: Cushman Foundation for Foraminiferal Research, Special Publication No. 40, 97 p.

———, GIBBARD, P. L., MILNE, G. A., and STARGARDT, J. M., 2005a, Holocene sea levels and palaeoenvironments of the Malay-Thai Peninsula, southeast Asia: The Holocene, v. 15, p. 1199-1213.

———, CORBETT, R., CULVER, S. J., EDWARDS, R. J., and HILLIER, C., 2006, Modern saltmarsh diatom distributions of the Outer Banks, North Carolina, and the development of a transfer function for high resolution reconstructions of sea level: Estuarine, Coastal, and Shelf Science, v. 69, p. 381-394.

———, THOMSON, K., WOODROFFE, S. E., WHITTAKER, J. E., and WRIGHT, M. W., 2005b, Contemporary foraminiferal distributions, Wakatobi National Park, southeast Sulawesi, Indonesia: Journal of Foraminiferal Research, v. 35, p. 1-14.

———, LARCOMBE, P., WOODROFFE, S. E., WHITTAKER, J. E., WRIGHT, M. W., and WYNN, C., 2003, Contemporary foraminiferal distributions of the Great Barrier Reef coastline, Australia: implications for sea-level reconstructions: Marine Geology, v. 198, p. 225-243.

HOTTINGER, L., 1977, Distribution of larger Peneroplidae, *Borelis* and Nummulitidae in the Gulf of Elat, Red Sea: Utrecht Micropalaeontological Bulletin, v. 15, p. 35-109.

HUGHEN, K. A., BAILLIE, M. G. L., BARD, E., BAYLISS, A., BECK, J. W., BERTRAND, C. J. H., BLACKWELL, P. G., BUCK, C. E., BURR, G. S., CUTLER, K. B., DAMON, P. E., EDWARDS, R. L., FAIRBANKS, R. G., FRIEDRICH, M., GUILDERSON, T. P., KROMER, B., MCCORMAC, F. G., MANNING, S. W., BRONK RAMSEY, C., REIMER, P. J., REIMER, R. W., REMMELE, S., SOUTHON, J. R., STUIVER, M., TALAMO, S., TAYLOR, F. W., VAN DER PLICHT, J., and WEYHENMEYER, C. E., 2004, Marine04 Marine radiocarbon age calibration, 26 - 0 ka BP: Radiocarbon, v. 46, p. 1059-1086.

HUGHES, G. W., 1977, Recent foraminifera from the Honiara Bay area, Solomon Islands: Journal of Foraminiferal Research, v. 7, p. 45-57.

JOHNSON, D. P., and SEARLE, D. E., 1984, Post-glacial seismic stratigraphy, central Great Barrier Reef, Australia: Sedimentology, v. 31, p. 335-352.

JOHNSON, D. P., BELPERIO, A. P., and HOPLEY, D., 1986, A Field-guide to Mixed Terrigenous-Carbonate Sedimentation in the Central Great Barrier Reef Province, Australia: Geological Society of Australia, Australasian Sedimentologists Group, Field Guide Series, no. 3, 174 p.

JONES, R. W., 1994, The Challenger Foraminifera: Oxford University Press, Oxford, 149 p.

JUGGINS, S., 2004, C2, Version 1.4, Newcastle University, UK, http://www.campus.ncl.ac.uk/staff/Stephen.Juggins/index.html.

KAUFMANN, G., and LAMBECK, K. 2002, Glacial isostatic adjustment and the radial viscosity profile from inverse modeling: Journal of Geophysical Research, v. 107, B11, 2280, doi:10.1029/2001JB000941.

LAMBECK , K., ESAT, T. M., and POTTER, E.-K., 2002, Links between climate and sea levels for the past three million years: Nature, v. 419, p. 199-206.

———, SMITHER, C., and JOHNSTON, P., 1998, Sea-level change, glacial rebound and mantle viscosity for northern Europe: Geophysical Journal International, v. 134, p. 102-144.

LANGER, M. R., and LIPPS, J. H., 2004, Foraminiferal distribution and diversity, Madang Reef and Lagoon, Papua New Guinea: Coral Reefs, v. 22, p. 143-154

LARCOMBE, P., and CARTER, R. M., 1998, Sequence architecture during the Holocene transgression: an example from the Great Barrier Reef Shelf, Australia: Sedimentary Geology, v. 117, p. 97-121.

———, and WOOLFE, K. J., 1999, Terrigenous sediments as influences upon Holocene nearshore coral reefs, central Great Barrier Reef, Australia: Australian Journal of Earth Sciences, v. 46, p. 141-154.

———, and———, 2004. Cyclone pumping, sediment partitioning and the development of the Great Barrier Reef shelf system: a review: Quaternary Science Reviews, v. 23, p. 107-135.

———, RIDD, P. V., PRYTZ, A., and WILSON, B., 1995b, Factors controlling suspended sediment on inner-shelf coral reefs, Townsville, Australia: Coral Reefs, v. 14, p. 163–171.

———, WOOLFE, K. J., DYE, J., GAGAN, M. K., and JOHNSON, D.P, 1995a, New evidence for episodic post-glacial sea-level rise, central Great Barrier Reef, Australia: Marine Geology, v. 127, p. 1-44.

LINE, J. M., TER BRAAK, C. J. F., and BIRKS, H. J. B., 1994, WACALIB version 3.3 - a computer program to reconstruct environmental variables from fossil assemblages by weighted averaging and to derive sample-specific errors of prediction: Journal of Paleolimnology, v. 10, p. 147-152.

LOEBLICH, A. R., and TAPPAN, H., 1994, Foraminifera of the Sahul Shelf and Timor Sea: Cushman Foundation for Foraminiferal Research Special Publication No. 31, 661 p.

VAN MARLE, L. J., 1988, Bathymetric distribution of benthic foraminifera on the Australian-Irian Jaya continental margin, Eastern Indonesia: Marine Micropaleontology, v. 13, p. 97-152.

MASSELL, S. R., and DONE, T. J., 1993, Effects of cyclone waves on massive coral assemblages on the GBR: meteorology, hydrodynamics and demography: Coral Reefs, v. 12, p. 153-166.

MASSEY, A. C., GEHRELS, W. R., CHARMAN, D. J., and WHITE, S. V., 2006, An intertidal foraminifera-based transfer function for reconstructing Holocene sea-level change in southwest England: Journal of Foraminiferal Research, v. 36, p. 215-232.

MAXWELL, W. G. H., 1968, Atlas of the Great Barrier Reef: Elsevier, Amsterdam, 258 p.

MCINTYRE, C., 1996, Holocene sedimentology and stratigraphy of Cleveland Bay, central Great Barrier Reef lagoon, Australia. Unpublished Masters Thesis, School of Earth Sciences, James Cook University, Townsville, Queensland, Australia, 185 p.

MORIGI, C., JORISSEN, F. J., FRATICELLI, S., HORTON, B. P., PRINCIPI, M., SABBATINI, A., CAPOTONDI, L., CURZI, P. V., and NEGRI, A., 2005, Benthic foraminiferal evidence for the formation of the Holocene mud-belt and bathymetrical evolution in the central Adriatic Sea: Marine Micropaleontology, v. 57, p. 25-49.

MILNE, G. A., LONG, A. J., and BASSETT, S. E., 2005, Modelling Holocene relative sea-level observations from the Caribbean and South America: Quaternary Science Reviews, v. 24, p. 1183-1202.

MITROVICA, J. X., and FORTE, A. M., 1997, Radial profile of mantle viscosity: results from the joint inversion of convection and postglacial rebound observables: Journal of Geophysical Research, v. 102, p. 2751-2769.

MURRAY, J. W., 1991, Ecology and Palaeoecology of Benthic Foraminifera: Longman Scientific and Technical, Harlow, England, 397 p.

———, and ALVE, E., 1999, Natural dissolution of modern shallow water benthic foraminifera: taphonomic effects on the palaeoecological record: Palaeogeography, Palaeoclimatology, Palaeoecology, Special Issue, v. 146, p. 195-209.

NATLAND, M. L., 1933, The temperature and depth distribution of some Recent and fossil foraminifera in the southern California region: Bulletin of the Scripps Institute of Oceanography, Technical Series, v. 3, p. 225-230.

NEIL, D. T., ORPIN, A. R., RIDD, P. V., and YU, B., 2002, Sediment yield and impacts from river catchments to the Great Barrier Reef lagoon: Marine and Freshwater Research, v. 53, p. 733-752.

OLIVER, J., 1978, The climatic environment of the Townsville area, *in* Hopley, D. (ed.), Geographical Studies of the Townsville Area, Monograph Series: Department of Geography, James Cook University of North Queensland, Occasional Paper, v. 2, p. 3-17.

ORPIN, A. R., HAIG, D. W., and WOOLFE, K. J., 1999a, Sedimentary and foraminiferal facies in Exmouth Gulf, in arid tropical northwestern Australia: Australian Journal of Earth Sciences, v. 46, p. 607.

———, RIDD, P. V., STEWART, L. K., 1999b, Assessment of the relative importance of major sediment-transport mechanisms within the central Great Barrier Reef lagoon: Australian Journal of Earth Science, v. 46, p. 883–896.

———, BRUNSKILL G. J., ZAGORSKIS I., and WOOLFE K. J., 2004, Patterns of mixed siliciclastic-carbonate sedimentation adjacent to a large dry-tropics river on the central Great Barrier Reef shelf, Australia: Australian Journal of Earth Sciences, v. 51, p. 665-683.

PATTERSON, R. T., GEHRELS, W. R., BELKNAP, D. F., and DALBY, A. P., 2004, The distribution of salt marsh foraminifera at Little Dipper Harbour New Brunswick, Canada: implications for development of widely applicable transfer functions in sea-level research: Quaternary International, v. 120, p. 185-194.

PELTIER, W. R. and FAIRBANKS, R. G., 2006, Global glacial ice volume and Last Glacial Maximum duration from an extended Barbados sea level record: Quaternary Science Reviews, v. 25, p. 3322-3337.

PHLEGER, F. B, 1960, Sedimentary patterns of microfaunas in northern Gulf of Mexico, *in* Shephard, F. P., Phleger, F. B and van Andel, T. H. (eds.), Recent Sediments, Northwest Gulf of Mexico: American Association of Petroleum Geologists, Tulsa, p. 267-301.

RADFORD, S. S., 1976, Depth distribution of Recent foraminifera in selected bays, Tobago Island, West Indies: Revista Española de Micropaleontología, v. 8, p. 219-238.

RENEMA, W., 2002, Larger foraminifera as marine environmental indicators: Scripta Geologica, v. 124, p. 1-263.

———, 2006, Large benthic foraminifera from the deep photic zone of a mixed siliciclastic-carbonate shelf off East Kalimantan, Indonesia: Marine Micropaleontology, v. 58, p. 73-82.

———, and TROELSTRA, S. R., 2001, Larger foraminifera distribution on a mesotrophic carbonate shelf in SW Sulawesi (Indonesia): Palaeogeography, Palaeoclimatology, Palaeoecology, v. 175, p. 125-147.

———, HOEKSEMA, B. W., and VAN HINTE, J. E., 2001, Larger benthic foraminifera and their distribution patterns on the Spermonde Shelf, South Sulawesi: Zoologische Verhandelingen, v. 334, p. 115-150.

SCOFFIN, T. P., AND TUDHOPE, A. W., 1985, Sedimentary environments of the central region of the Great Barrier Reef of Australia: Coral Reefs, v. 4, p. 81-93.

SCOTT, D. B., and HERMELIN, J. O., 1993. A device for splitting of micropaleontological samples in liquid suspension: Journal of Paleontology, v. 67, p. 151-154.

———, and MEDIOLI, F. S., 1978, Vertical zonation of marsh foraminifera as accurate indicators of former sea levels: Nature, v. 272, p. 528-531.

———, ———, and SCHAFER, C. T., 2001, Monitoring in Coastal Environments using Foraminifera and Thecamoebian indicators: Cambridge University Press, Cambridge, 177 p.

SEN GUPTA, B. K., 1977, Depth-distribution of modern benthic foraminifera on continental shelves of the world ocean: Indian Journal of Earth Science, v. 4, p. 60-83.

———, 1982, Ecology of benthic foraminifera, *in* Broadhead, T. W. (ed.), Foraminifera: Notes for a Short Course: University of Tennessee, Department of Geological Sciences, Studies in Geology, v. 6, p. 37-50.

SHENNAN, I., and MILNE, G. A., 2003, Sea-level observations around the Last Glacial Maximum from the Bonaparte Gulf, NW Australia: Quaternary Science Reviews, v. 22, p. 1543-1547.

SLOSS, C. R., JONES, B. G., MURRAY-WALLACE, C. V., and MCCLENNEN, C. E., 2005, Holocene sea level fluctuations and the sedimentary evolution of a barrier estuary: Lake Illawarra, New South Wales, Australia: Journal of Coastal Research, v. 21, p. 943-959.

SOUTHALL, K. E., GEHRELS, W. R., and HAYWARD, B. W., 2006, Foraminifera in a New Zealand salt marsh and their suitability as sea-level indicators: Marine Micropaleontology, v. 60, p. 167-179.

TOSCANO, M. A., and MACINTYRE, I. G., 2003, Corrected western Atlantic sea-level curve for the last 11,000 years based on calibrated ^{14}C dates from *Acropora palmata* framework and intertidal mangrove peat: Coral Reefs, v. 22, p. 257-270.

TUSHINGHAM, A. M., and PELTIER, W. R., 1991, ICE-3G: A new global model of late Pleistocene deglaciation based on geophysical predictions of postglacial relative sea level change: Journal of Geophysical Research, v. 96, p. 4497-4523.

UCHIO, T., 1962, Influence of the River Shinano on foraminifera and sediment grain size distributions: Publications of the Seto Marine Biological Laboratory, v. 10, p. 363-392.

———, 1967, Foraminiferal assemblages in the vicinity of the Seto Marine Biological Laboratory, Shirahama-Cho, Wakayama-Ken, Japan: Publications of the Seto Marine Biological Laboratory, v. 15, p. 399-417.

ULM, S., 2002, Marine and estuarine reservoir effects in Central Queensland, Australia: Determination of ΔR values: Geoarchaeology, v. 17, p. 319-348.

WANG, P., and CHAPPELL, J., 2001, Foraminifera as Holocene environmental indicators in the South Alligator River, Northern Australia: Quaternary International, v. 83-85, p. 47-62.

WOLANSKI, E., 1994, Physical Oceanographic Processes of the Great Barrier Reef, CRC Press, Boca Raton, 194 p.

WOODROFFE, S. A., 2006 Holocene relative sea-level changes in Cleveland Bay, North Queensland, Australia: Unpublished Ph.D. Thesis, University of Durham, Durham, UK, 155 p.

———, HORTON, B. P., LARCOMBE, P., and WHITTAKER, J. E., 2005, Intertidal mangrove foraminiferal from the Central Great Barrier Reef Shelf, Australia: implications for sea-level reconstructions: Journal of Foraminiferal Research, v. 35, p. 259-270.

YASSINI, I., and JONES, B. G., 1995, Foraminiferida and ostracoda from estuarine and shelf environments on the southeastern coast of Australia: University of Wollongong Press, Wollongong, 484 p.

YOKOYAMA, Y., LAMBECK, K., DE DECKKER, P., JOHNSTON, P., and FIFIELD, L. K., 2000, Timing of the Last Glacial Maximum from observed sea-level minima: Nature, v. 406, p. 713–716.

TABLES

Table 1. Sea-level index points from Cleveland Bay collected on cruise numbers KG857, KG902, KG911 and KG912b aboard R/V *James Kirby*. All mean $^{14}C \pm 1\sigma$ dates are calibrated using using OxCal (ver 3.10; Bronk Ramsey, 2005) and 2σ. * We have used the marine04.14c dataset (Hughen and others, 2004) and ΔR of -19 ± 38 years (Ulm, 2002). The water depth is predicted using the subtidal transfer function. Relative sea level (RSL) is calculated from the combination of elevation (m AHD) and water depth. The RSL error calculation includes the sum of all the quantified, or estimated, height errors; these include transfer function error, sample elevation error and sample thickness [total error = $\sqrt{(e_1^2 + e_2^2 + \ldots e_n^2)}$].

Table 2. Apparent errors of estimation and prediction errors for components 1-5 of the WA-PLS subtidal foraminiferal-based transfer functions. Root-mean square of the error of prediction (RMSEP) and the squared correlation (r^2).

Table 1

Sample	**Dated material**	**Laboratory code**	**^{14}C age BP ±1σ**	**Calibrated age range**	**RSL (m AHD)**
911v15*	*Marginopora*	GAK2211	2100 ± 164	2098 - 1326	-0.6 ± 4.4
902v102*	*Bursa rana*	GAK2453	2270 ± 144	2283 - 1560	-0.3 ± 3.7
902v121*	*Vexillium amanda*	GAK2449	2860 ± 213	3183 - 2096	0.6 ± 3.9
911v16*	*Ostrea* sp.	GAK2215	4200 ± 78	4551 - 4064	0.9 ± 3.9
911v8*	Bivalves	GAK2443	6153 ± 95	6863 - 6379	1.7 ± 3.9
857dv16	Plant macro	GAK7224	6310 ± 170	7600 - 6750	1.7 ± 3.8
912bv4*	*Austromactra dissimillis*	GAK2444	7741 ± 97	8413 - 7993	-2.9 ± 3.8
902v113	Organic mud	GAK3553	7840 ± 170	9150 - 8300	-5.6 ± 4.3
902v106	Organic mud	GAK3550	8110 ± 210	9550 - 8500	-5.8 ± 4.1
911v11*	Gastropod	GAK2210	8380 ± 125	9330 - 8598	-8.9 ± 4.5

Table 2.

Component	Apparent (r^2)	Apparent RMSE (m)	Prediction (r^2)	Prediction RMSEP (m)
1	0.87	3.83	0.83	4.42
2	0.94	2.50	0.90	3.50
3	0.96	2.11	0.89	3.64
4	0.97	1.95	0.87	3.89
5	0.97	1.76	0.85	4.27

FIGURES

Fig. 1 Location map of the study area showing (a) the Great Barrier Reef coastline Australia, contemporary sites of (b) Cleveland Bay and (c) Bowling Green Bay and (d) vibracore sites of Cleveland Bay. The samples were collected on cruise numbers KG857, KG902, KG911 and KG912b aboard R/V *James Kirby*.

Fig. 2 Relative foraminiferal abundance (%) of the five most abundant foraminiferal species from Cleveland Bay (a) Transect 1 and (b) Transect 2. Water depths and distance along the transect (km) are indicated.

Fig. 3 (a) Unconstrained cluster analysis based on unweighted Euclidean distances showing the contemporary foraminiferal assemblages versus order of samples on dendrogram, (b) detrended correspondence analysis (sample label is shown) and (c) bathymetric distribution of Cleveland Bay transects 1 and 2. Only species with relative abundances greater than 10% in one or more samples are shown.

Fig. 4 Relative foraminiferal abundance (%) of the six most abundant foraminiferal species from Bowling Green Bay. Water depths and distance along thetransect (m) are indicated.

Fig. 5 (a) Unconstrained cluster analysis based on unweighted Euclidean distances showing the contemporary foraminiferal assemblages versus order of samples on dendrogram, (b) detrended correspondence analysis (sample labels are shown) and (c) bathymetric distribution of Bowling Green Bay. Only species with relative abundances greater than 10% in one sample are shown.

Fig. 6 Detrended correspondence analysis of the combined dataset from Cleveland Bay and Bowling Green Bay.

Fig. 7 (a) Scatter plots and (b) residuals showing the relationship of the regression of observed water depths (m) versus subtidal foraminiferal-predicted water depths using WA-PLS from Cleveland Bay and Bowling Green Bay.

Fig. 8 Scatter plots and *r* values showing the relationship between subtidal foraminiferal assemblages and water depth from Cleveland Bay and Bowling Green Bay. The *r* values in bold show statistically significant relationships ($p = 0.01$ and $df = 41$). The lowess curves (locally weighted scatter plot smoothing) are shown.

Fig. 9 Dominant species in Cleveland Bay vibracores. Only species with relative abundances greater than 10% are shown. Water depths (m) predicted using WA-PLS with associated error ranges are shown.

Fig. 10 Holocene sea-level reconstructions for Cleveland Bay using the subtidal foraminiferal-based transfer function. Two geophysical model predictions are shown as dashed lines, which correspond to outer shell, or lithosphere thickness of 120 km and 96 km. The sea-level index points show calibrated age ranges and the relative sea-level error (see Table 1).

PLATE 1

1 *Quinqueloculina pseudoreticulata* (Parr): **a** side view, **b** apertural view; x 130. **2** *Quinqueloculina venusta* (Karrer): **a** side view, **b** apertural view; x 100. **3** *Triloculina oblonga* (Montagu): **a** side view, **b** apertural view; x 100. **4** *Dendritina striata* (d'Orbigny): **a** side view, **b** apertural view; x 110. **5** *Pararotalia venusta* (Brady): **a** umbilical view, **b** spiral view; x 170. **6** *Ammonia aoteana* (Finlay): **a** side view, **b** spiral view, **c** umbilical view; x 250. **7** *Ammonia tepida* (Cushman): **a** umbilical view, **b** spiral view; x 150. **8** *Elphidium albanii* (Hayward): **a** side view, **b** edge view; x 120. **9** *Elphidium hispidulum* (Cushman): **a** side view, **b** edge view; x 300. **10** *Planispirinella exigua* (Brady): **a** side view, **b** apertural view; x 200. **11** Amphistegina *lessonii* (d'Orbigny): side view; x 80. **12** *Operculina complanata* (Defrance): side view; x 50.

APPENDIX A

Foraminiferal taxonomy for those species mentioned in the text.

Species	Citation
Amphistegina lessonii (d'Orbigny)	*Amphistegina lessonii* d'Orbigny, 1826, p. 304, no. 3, pl. 17, figs 1-4. Bock, 1971, p. 58, pl. 21, fig. 10.
Dendritina striata (d'Orbigny)	*Spirolina striata* d'Orbigny, 1850. *Dendritina striata* Hofker. 1951, pl. 1, figs 38-39.
Elphidium albanii (Hayward)	*Elphidium albanii* Hayward, 1997, pl. 6, figs 1-5. *Cribrononion oceanicus* (Cushman). Albani, 1978, p. 387, fig 9B.
Elphidium hispidulum (Cushman)	*Elphidium hispidulum* Cushman. 1936, p.83, pl. 14, fig. 13. *Elphidium reticulosum* (Cushman). Loeblich and Tappan, 1994, p. 169, pl. 382, figs.1-5.
Operculina complanata (Defrance)	*Lenticulites complanata* (Defrance). Defrance, 1822, p.453. *Operculina complanata* (Defrance). d'Orbigny, 1826, p. 281, pl. XIV, figs 7-10.
Pararotalia venusta (Brady)	*Rotalia venusta* Brady, 1884, pl.108, fig. 2c
Planispirinella exigua (Brady)	*Hauerina exiqua* Brady, 1879, p. 267
Quinqueloculina pseudoreticulata (Parr)	*Quinqueloculina pseudoreticulata* Parr, 1941, p. 305. Brady, 1884, p. 177, pl. 9 figs 2-3
Quinqueloculina venusta (Karrer)	*Quinqueloculina venusta* Karrer, 1868, p. 147, pl. 2, fig. 6.
Triloculina oblonga (Montagu)	*Verniculum oblongum* Montagu, 1803, p. 522, pl. 14, fig. 9. *Triloculina oblonga* (Montagu, 1803), figs 5.16, 5.17

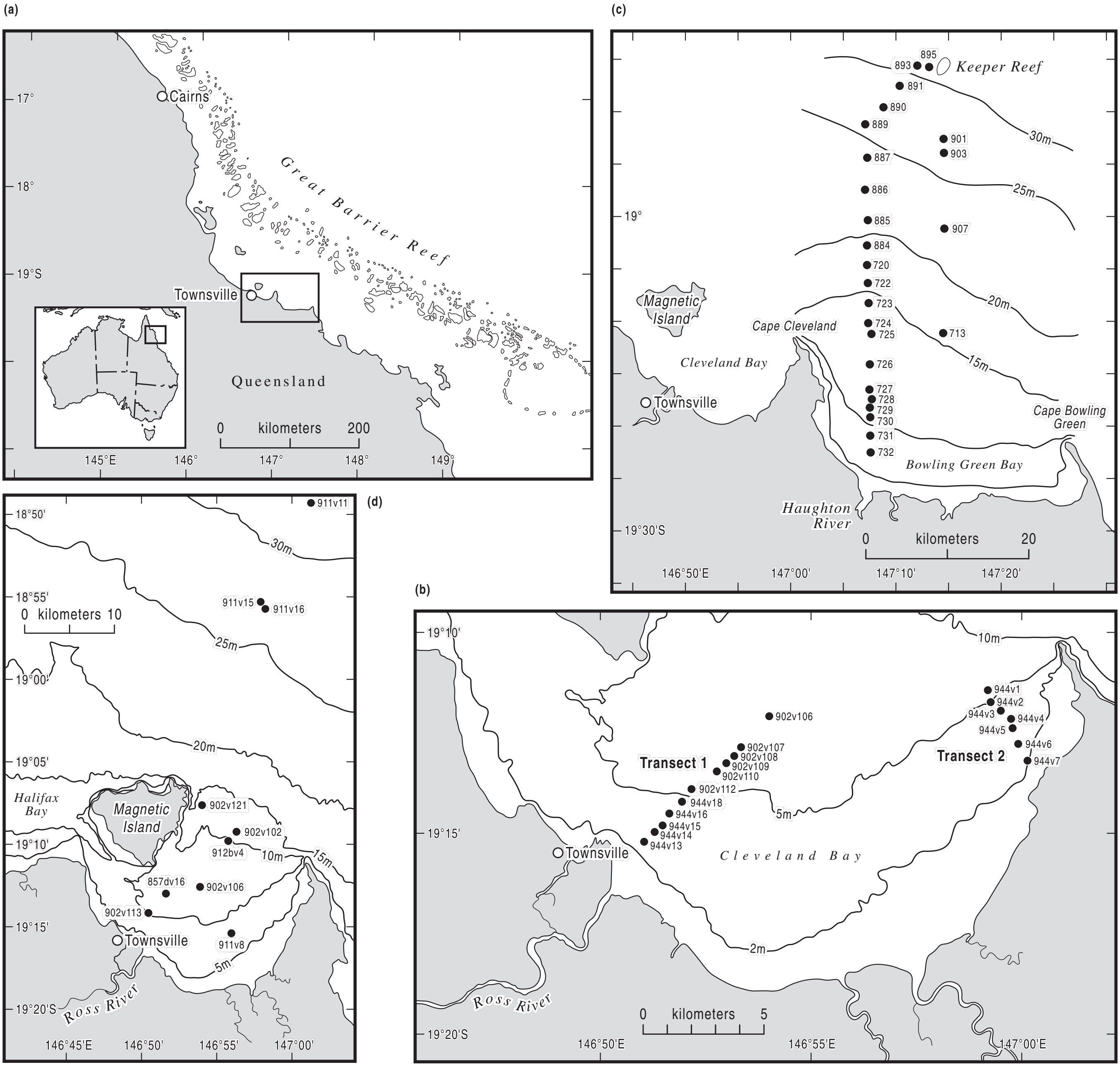
(a)
Cairns
Great Barrier Reef
Townsville
Queensland
17°
18°
19°S
0 kilometers 200
145°E
146°
147°
148°
149°
(c)
Keeper Reef
895
893
891
890
889
901
903
887
886
885
907
884
720
722
723
724
725
713
726
727
728
729
730
731
732
30m
25m
20m
15m
19°
Magnetic Island
Cape Cleveland
Cleveland Bay
Townsville
Cape Bowling Green
Bowling Green Bay
Haughton River
19°30'S
0 kilometers 20
146°50'E
147°00'
147°10'
147°20'
(d)
911v11
18°50'
30m
18°55'
911v15
911v16
0 kilometers 10
25m
19°00'
20m
19°05'
Halifax Bay
Magnetic Island
902v121
902v102
912bv4
10m
15m
19°10'
857dv16
902v106
902v113
19°15'
Townsville
911v8
5m
19°20'S
Ross River
146°45'E
146°50'
146°55'
147°00'
(b)
19°10'
10m
944v1
944v2
944v3
944v4
944v5
944v6
944v7
902v106
902v107
902v108
902v109
902v110
902v112
944v18
944v16
944v15
944v14
944v13
Transect 1
Transect 2
5m
19°15'
Townsville
Cleveland Bay
2m
Ross River
0 kilometers 5
19°20'S
146°50'E
146°55'E
147°00'E

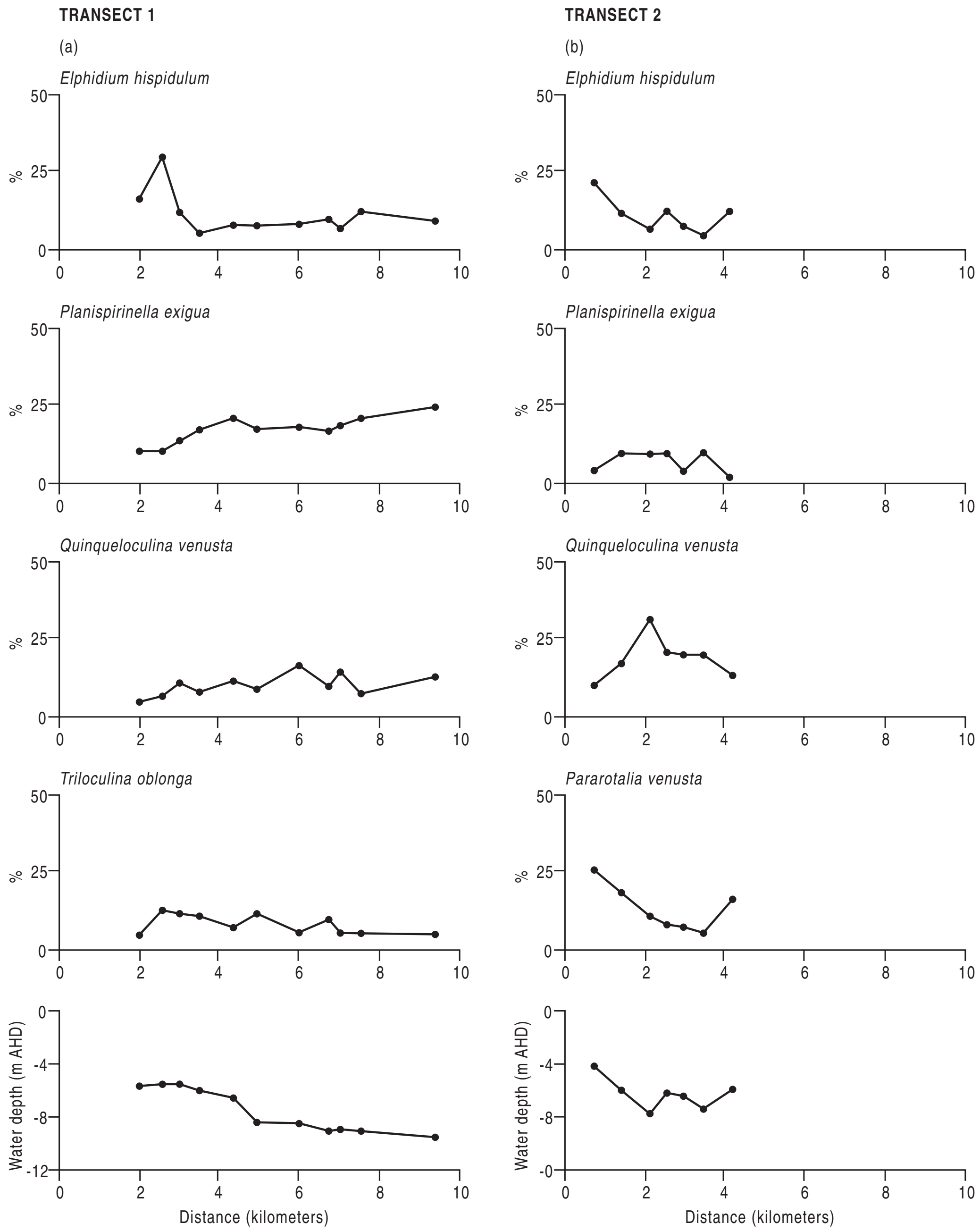
TRANSECT 1
(a)
Elphidium hispidulum
Planispirinella exigua
Quinqueloculina venusta
Triloculina oblonga
%
Water depth (m AHD)
Distance (kilometers)
TRANSECT 2
(b)
Elphidium hispidulum
Planispirinella exigua
Quinqueloculina venusta
Pararotalia venusta
%
Water depth (m AHD)
Distance (kilometers)

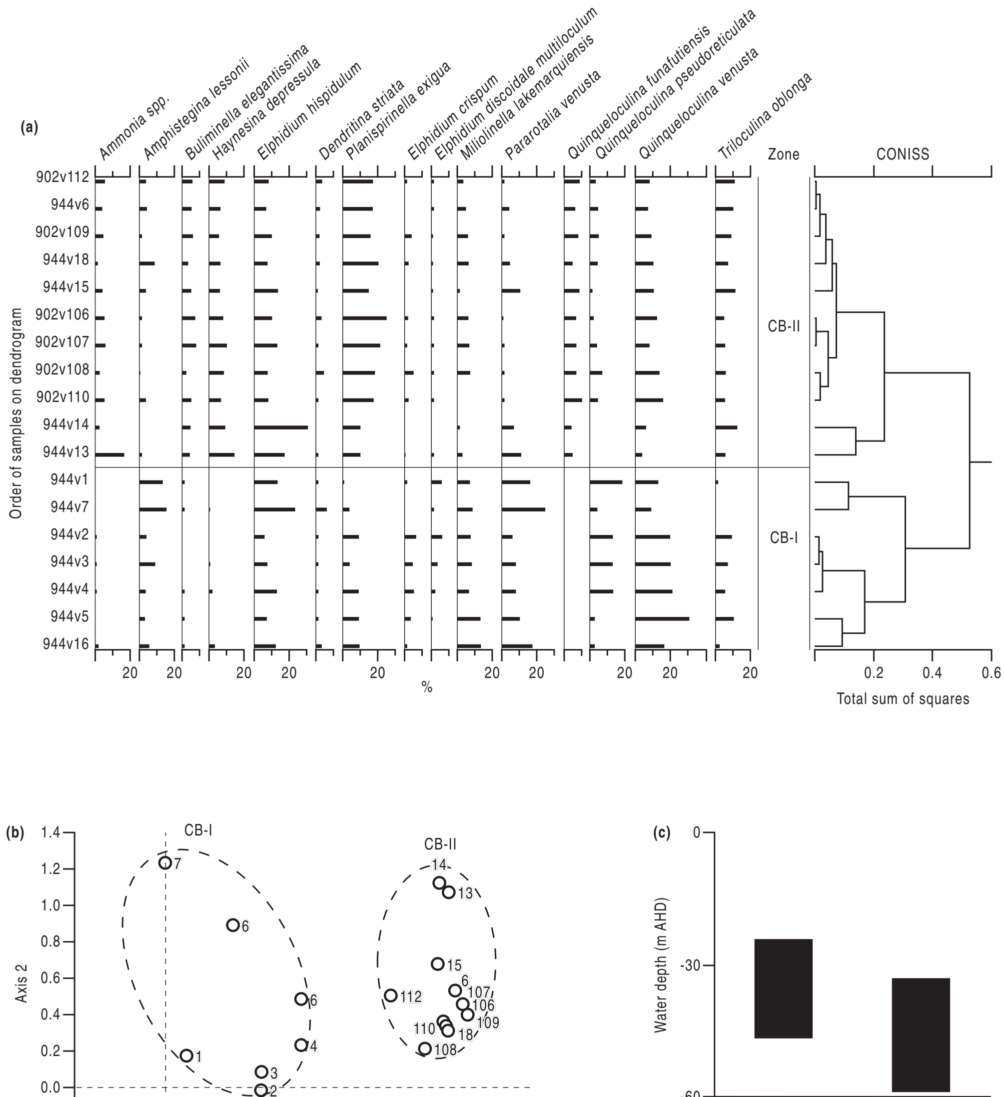
(a)
Ammonia spp.
Amphistegina lessonii
Buliminella elegantissima
Haynesina depressula
Elphidium hispidulum
Dendritina striata
Planispirinella exigua
Elphidium crispum
Elphidium discoidale multiloculum
Miliolinella lakemarquiensis
Pararotalia venusta
Quinqueloculina funafutiensis
Quinqueloculina pseudoreticulata
Quinqueloculina venusta
Triloculina oblonga
Zone
CONISS
Order of samples on dendrogram
902v112
944v6
902v109
944v18
944v15
902v106
902v107
902v108
902v110
944v14
944v13
944v1
944v7
944v2
944v3
944v4
944v5
944v16
CB-II
CB-I
20
%
0.2
0.4
0.6
Total sum of squares
(b)
CB-I
CB-II
Axis 2
Axis 1
(c)
Water depth (m AHD)
0
-30
-60
Zone

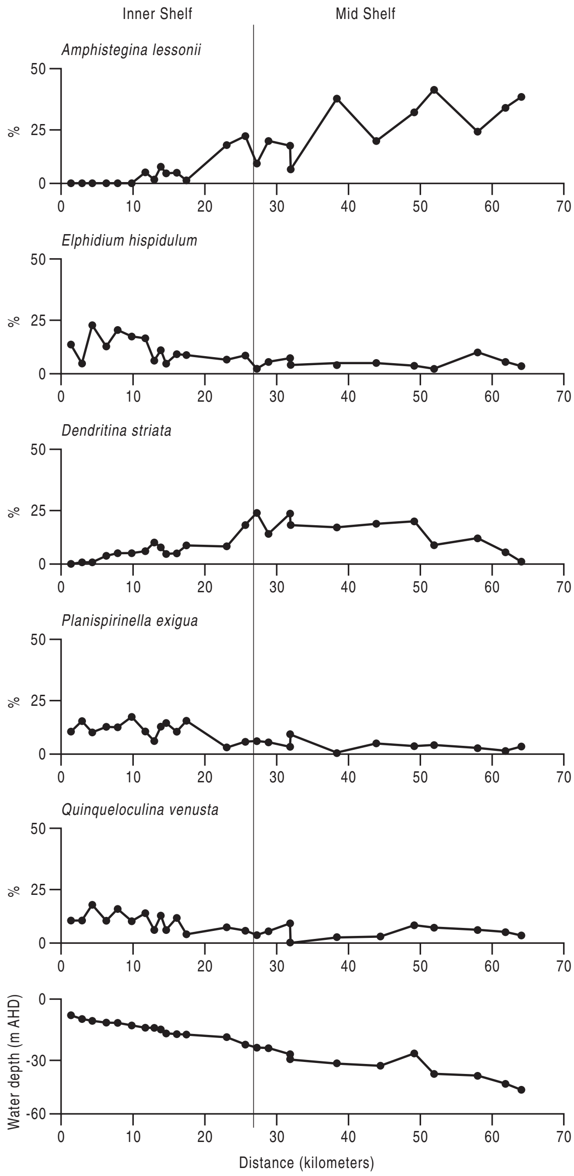

Inner Shelf
Mid Shelf
Amphistegina lessonii
Elphidium hispidulum
Dendritina striata
Planispirinella exigua
Quinqueloculina venusta
%
0
25
50
0
10
20
30
40
50
60
70
Water depth (m AHD)
0
-30
-60
Distance (kilometers)

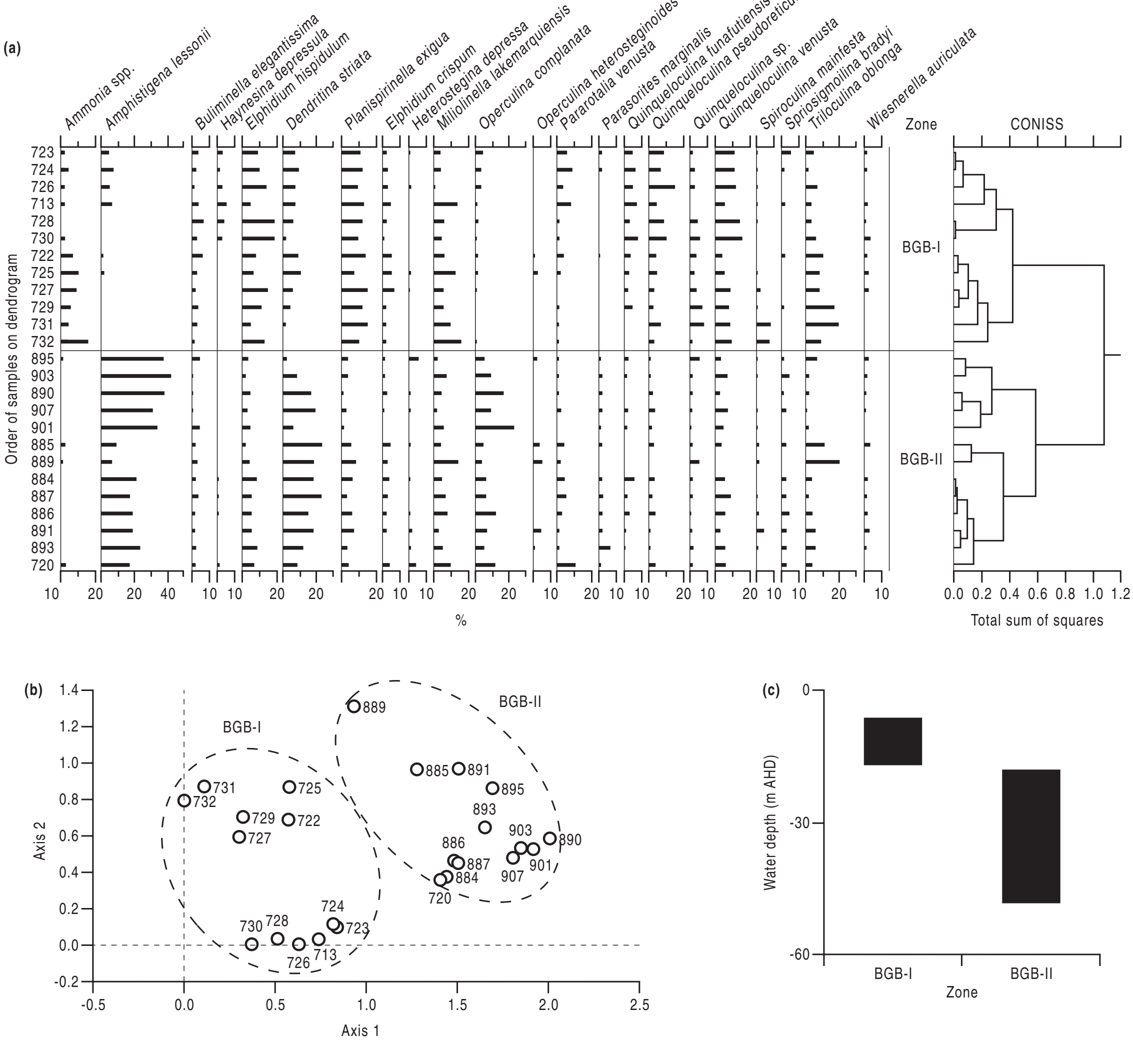
(a)
Ammonia spp.
Amphistigena lessonii
Buliminella elegantissima
Haynesina depressula
Elphidium hispidulum
Dendritina striata
Planispirinella exigua
Elphidium crispum
Heterostegina depressa
Miliolinella lakemarquiensis
Operculina complanata
Operculina heterosteginoides
Pararotalia venusta
Parasorites marginalis
Quinqueloculina funafutiensis
Quinqueloculina pseudoreticulata
Quinqueloculina sp.
Quinqueloculina venusta
Spiroculina manifesta
Spriosigmoilina bradyi
Triloculina oblonga
Wiesnerella auriculata
Zone
CONISS
Order of samples on dendrogram
723
724
726
713
728
730
722
725
727
729
731
732
895
903
890
907
901
885
889
884
887
886
891
893
720
BGB-I
BGB-II
%
Total sum of squares
0.0 0.2 0.4 0.6 0.8 1.0 1.2
(b)
Axis 1
Axis 2
BGB-I
BGB-II
(c)
Water depth (m AHD)
Zone
BGB-I
BGB-II

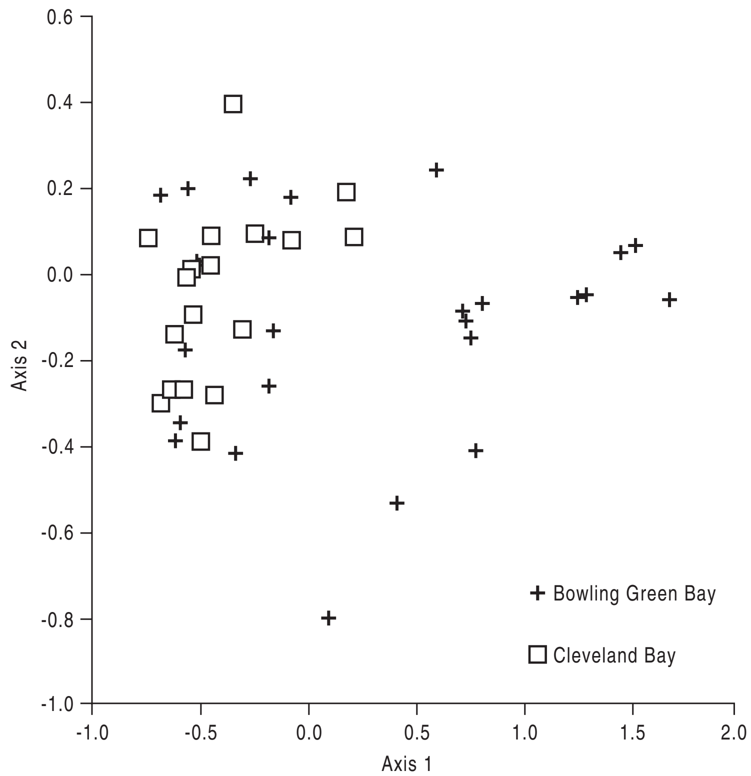
0.6
0.4
0.2
0.0
-0.2
-0.4
-0.6
-0.8
-1.0
Axis 2
-1.0
-0.5
0.0
0.5
1.0
1.5
2.0
Axis 1
Bowling Green Bay
Cleveland Bay

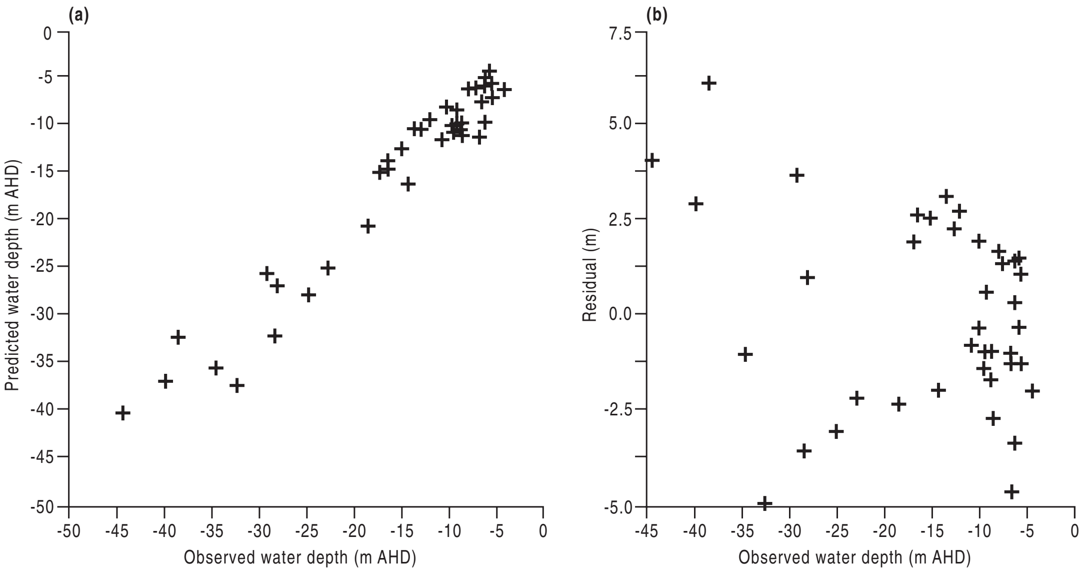

(a)
Predicted water depth (m AHD)
Observed water depth (m AHD)
0
-5
-10
-15
-20
-25
-30
-35
-40
-45
-50
(b)
Residual (m)
Observed water depth (m AHD)
7.5
5.0
2.5
0.0
-2.5
-5.0

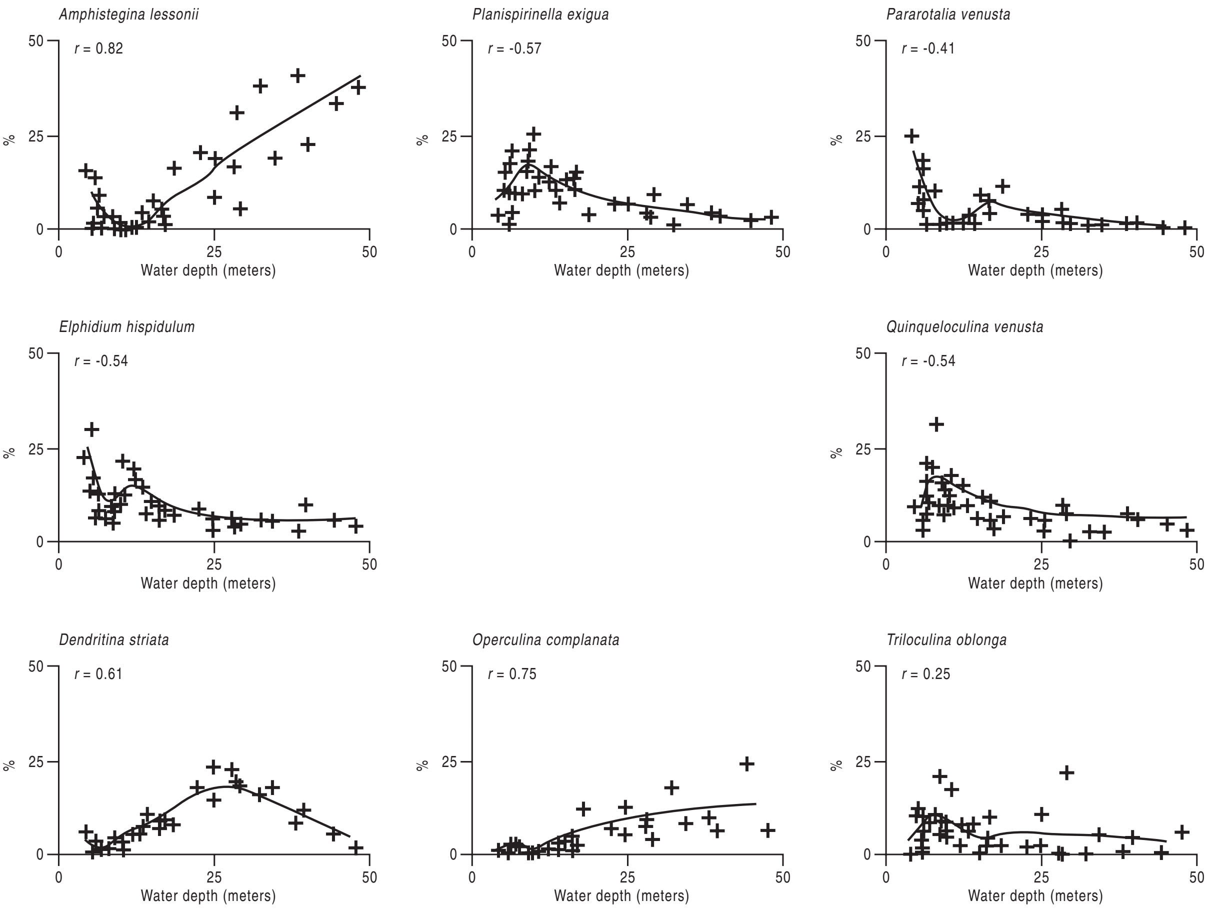
Amphistegina lessonii
r = 0.82
Planispirinella exigua
r = -0.57
Pararotalia venusta
r = -0.41
Elphidium hispidulum
r = -0.54
Quinqueloculina venusta
r = -0.54
Dendritina striata
r = 0.61
Operculina complanata
r = 0.75
Triloculina oblonga
r = 0.25
%
0
25
50
Water depth (meters)

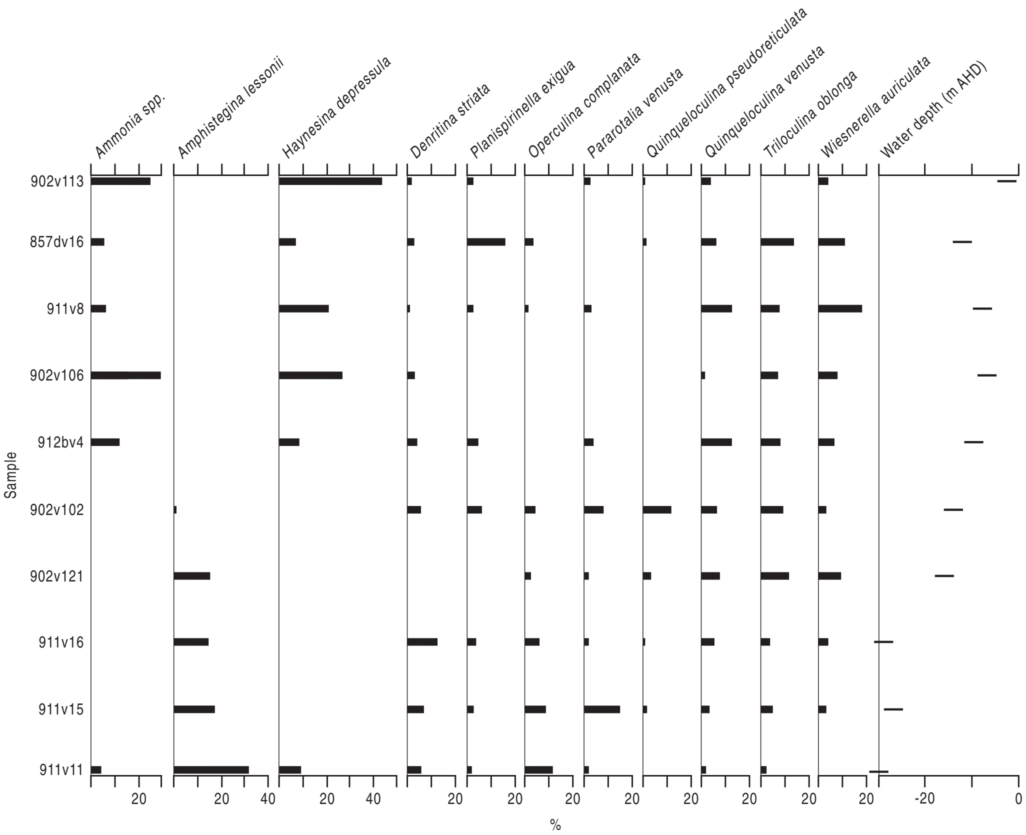
Ammonia spp.
Amphistegina lessonii
Haynesina depressula
Denritina striata
Planispirinella exigua
Operculina complanata
Pararotalia venusta
Quinqueloculina pseudoreticulata
Quinqueloculina venusta
Triloculina oblonga
Wiesnerella auriculata
Water depth (m AHD)
902v113
857dv16
911v8
902v106
912bv4
902v102
902v121
911v16
911v15
911v11
Sample
20
20
40
20
40
20
20
20
20
20
20
20
20
-20
0
%

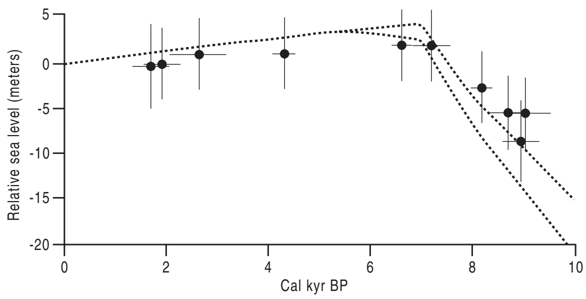

5
0
-5
-10
-15
-20
Relative sea level (meters)
0
2
4
6
8
10
Cal kyr BP

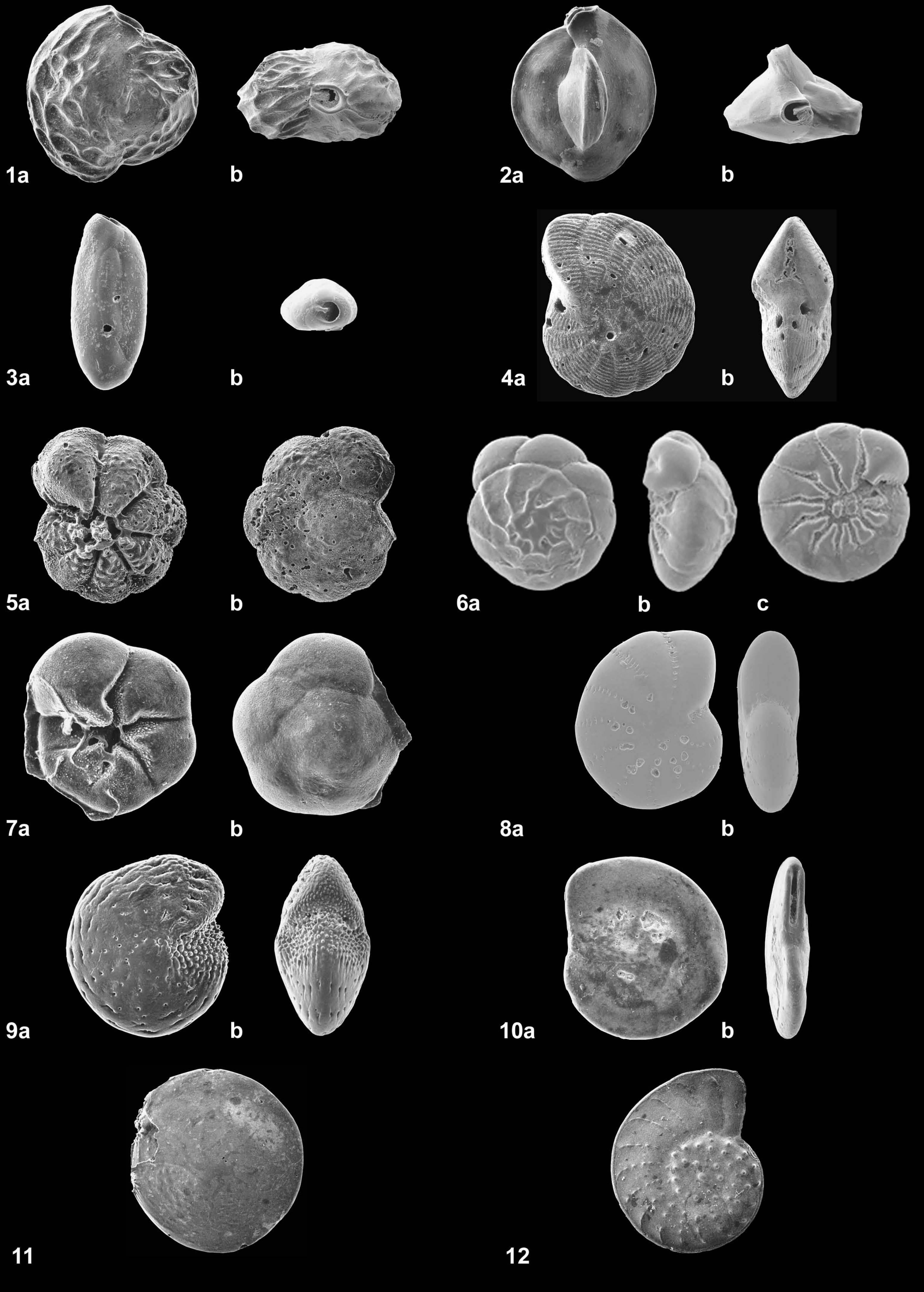
1a
b
2a
b
3a
b
4a
b
5a
b
6a
b
c
7a
b
8a
b
9a
b
10a
b
11
12